Supplementary Information (SI) Appendix

Minimal and RNA-free RNase P in *Aquifex aeolicus*

Astrid I. Nickel[1], Nadine B. Wäber[1], Markus Gößringer[1], Marcus Lechner[1], Uwe Linne[2], Ursula Toth[3], Walter Rossmanith[3], Roland K. Hartmann[1†]

Table of Contents

Three step purification procedure

Anion exchange chromatography (AEC)

After cell lysis using a French press and ultracentrifugation, the supernatant was purified by anion exchange chromatography (AEC) using a Diethylaminoethyl (DEAE) Sepharose Fast Flow column (GE Healthcare). RNase P activity eluted in step three at approximately 340 mM ammonium chloride.

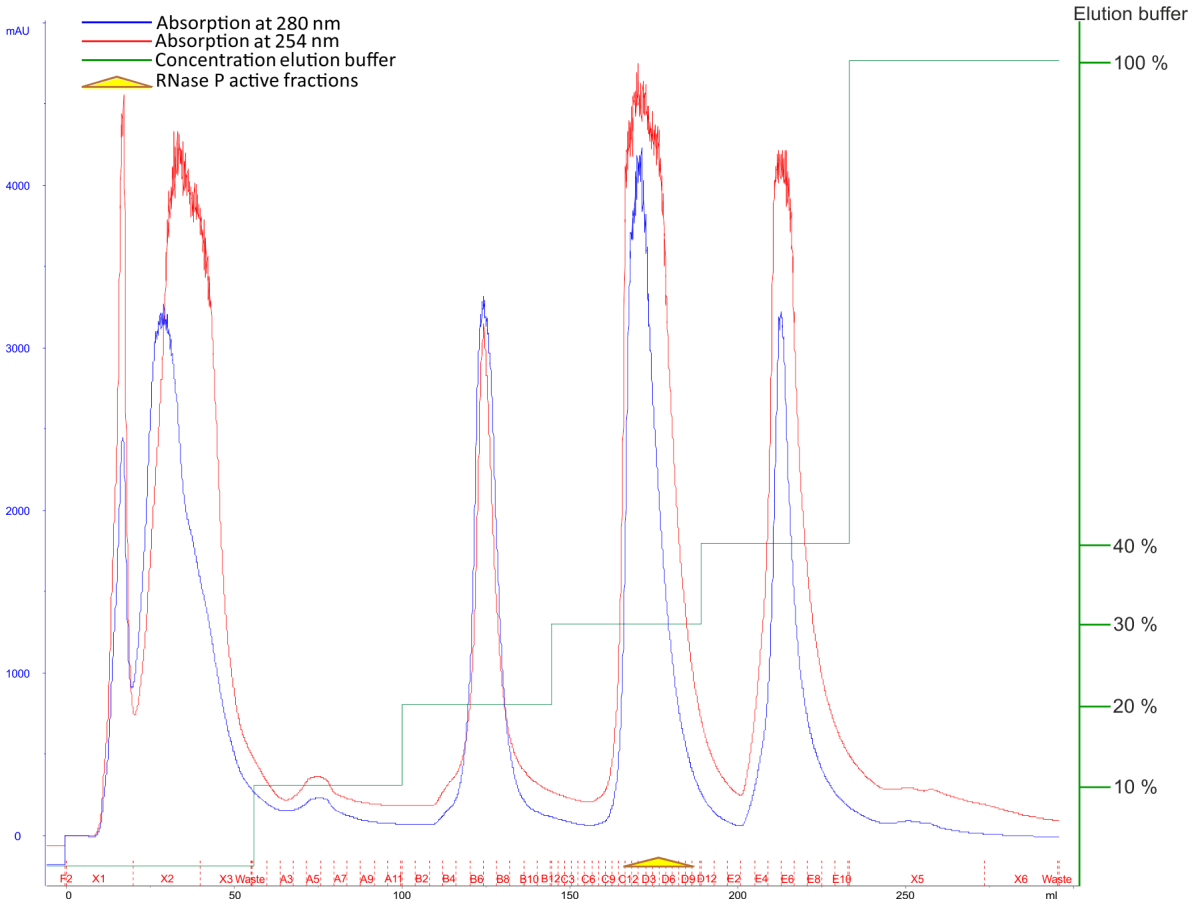

Figure S1: AEC (DEAE) chromatography of *A. aeolicus* cell lysates. Purification was performed by applying a step gradient, starting with buffer A60 containing 60 mM ammonium chloride. In each elution step the concentration of elution buffer A1000 containing 1 M NH_4Cl was increased by 10%. Eluted fractions were tested for RNase P activity. Active fractions eluted in step 3 (marked with a yellow triangle) at 30% elution buffer.

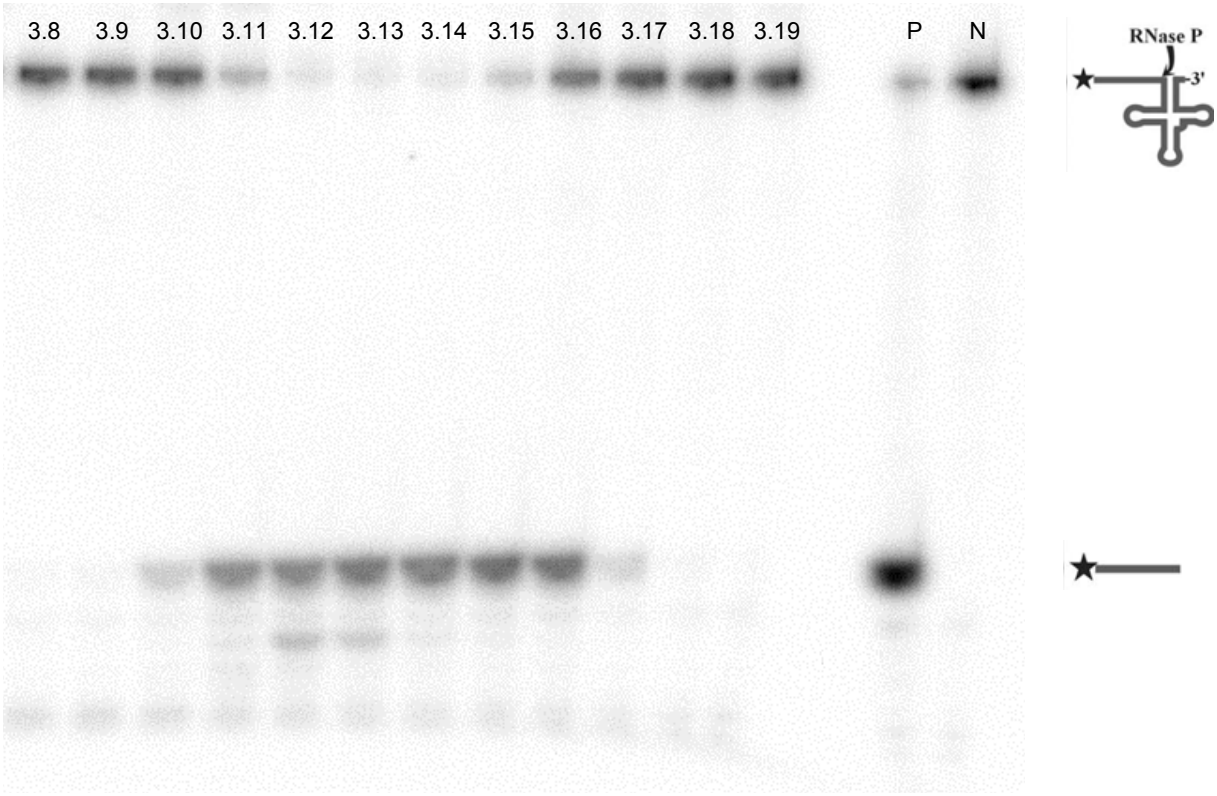

Figure S2: DEAE fractions were tested for RNase P activity and analyzed on a 20% denaturing PAA gel containing 8 M urea. 5'-[^{32}P]-labeled pre-tRNA^{Gly} was incubated with 5 µl of each fraction eluted in step 3 of the AEC. 3.8 – 3.19: fractions collected in step 3. P: positive control, cleavage of pre-tRNA^{Gly} by *E. coli* P RNA in the presence of 10 mM $Mg(OAc)_2$); N: negative control (ddH_2O instead of enzyme). Highest RNase P activity was present in fractions 3.12 – 3.14. For assay details, see Suppl. Materials and Methods below, paragraph "Processing assays".

Hydrophobic interaction chromatography (HIC)

After anion exchange chromatography, DEAE fractions with substantial RNase P activity were pooled and concentrated using Amicon Ultra-15 centrifugal filters. The concentrated fractions were adjusted to buffer A2, which corresponds to buffer A60 but additionally containing 1 M $(NH_4)_2SO_4$, and loaded onto a Phenyl Sepharose column. Elution was again performed stepwise, starting with buffer A2 and replacing it to 20, 40, 60, 80 and 100% with buffer A60 [no $(NH_4)_2SO_4$)] in elution steps 1 to 5. Fractions with RNase P activity eluted mainly in steps 3 and 4 at 0.4 and 0.2 M $(NH_4)_2SO_4$, respectively. In the following, RNase P fractions eluting from the HIC column at 0.4 M and 0.2 M $(NH_4)_2SO_4$ were denoted as "$HIC_{0.4}$" and "$HIC_{0.2}$", respectively. Only minor RNase P activity was detectable when the $HIC_{0.4}$ and $HIC_{0.2}$ fractions were tested directly after elution. However, activity could be rescued by subsequent dialysis against buffer A60. For fractions that eluted during HIC in step 5 with no $(NH_4)_2SO_4$ in the elution buffer (fractions denoted as "HIC_0"), dialysis could be omitted and RNase P activity was detected after pooling and concentration of several HIC_0 fractions, likely due to low levels of RNase P activity in individual fractions from single column runs.

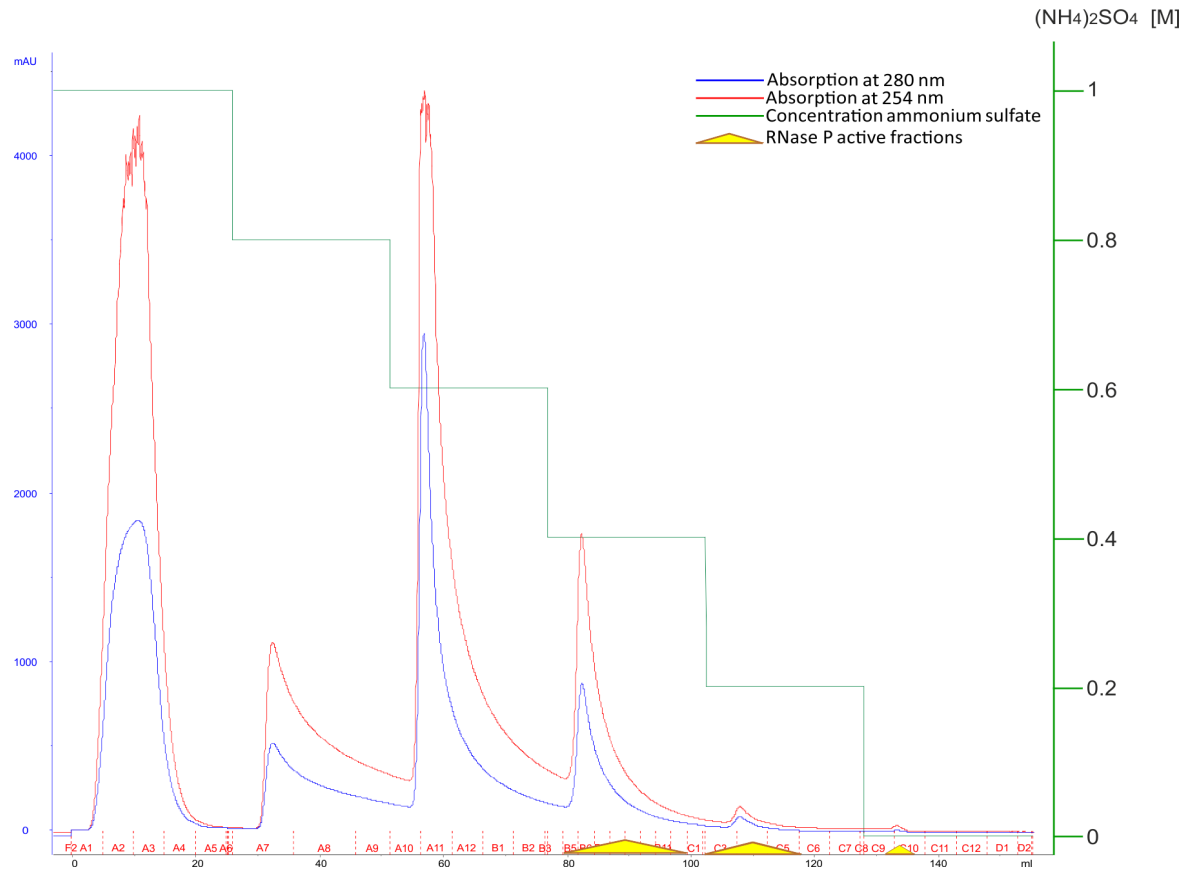

Figure S3: Chromatogram of the Phenyl Sepharose (HIC) column. After sample loading, the ammonium sulfate concentration was decreased from 1 to 0 M in 0.2 M steps. Yellow triangles indicate fractions with RNase P activity that eluted at 0.4 M $(NH_4)_2SO_4$ in step 3 ($HIC_{0.4}$), at 0.2 M $(NH_4)_2SO_4$ in step 4 ($HIC_{0.2}$) and in the last step without $(NH_4)_2SO_4$ (HIC_0).

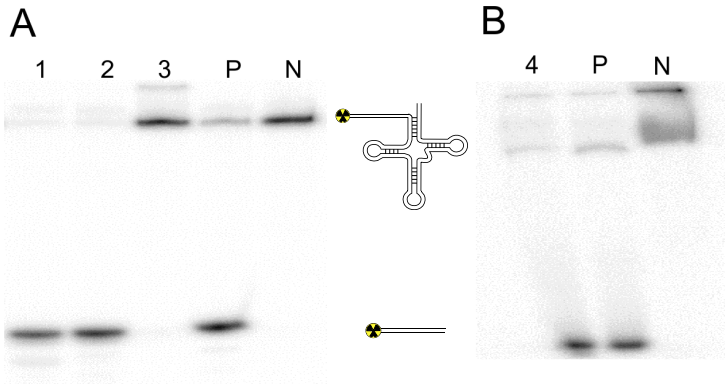

Figure S4: (**A**) RNase P activity test of HIC fractions that eluted at 0.2 M ($HIC_{0.2}$; lane 1), 0.4 M ($HIC_{0.4}$; lane 2) and 0.6 M ($HIC_{0.6}$; lane 3) $(NH_4)_2SO_4$. For the RNase P activity test, respective fractions of two independent HIC purifications were pooled, dialyzed and concentrated. (**B**) RNase P activity in the HIC fraction that eluted in step 5 at 0 M $(NH_4)_2SO_4$ (HIC_0; lane 4). For the RNase P activity test, corresponding fractions of 4 independent HIC purifications were pooled and concentrated. P: positive control, cleavage of pre-$tRNA^{Gly}$ by *E. coli* P RNA as in Fig. S2; N: negative control (ddH_2O instead of enzyme).

Size exclusion chromatography (SEC)

In the third purification step, HIC fractions with RNase P activity were purified by size exclusion chromatography (SEC). Since the elution profiles of the fractions $HIC_{0.4}$ and $HIC_{0.2}$ were different, both fractions were (after dialysis and concentrating) purified separately by size exclusion chromatography using a Superose 6 column. The eluted fractions containing RNase P activity were termed "$SEC_{0.4}$" and "$SEC_{0.2}$", respectively. The separation of fractions with RNase P activity from the bulk of proteins was more efficient when applying the concentrated $HIC_{0.2}$ relative to the $HIC_{0.4}$ fractions.

$SEC_{0.2}$ chromatogram

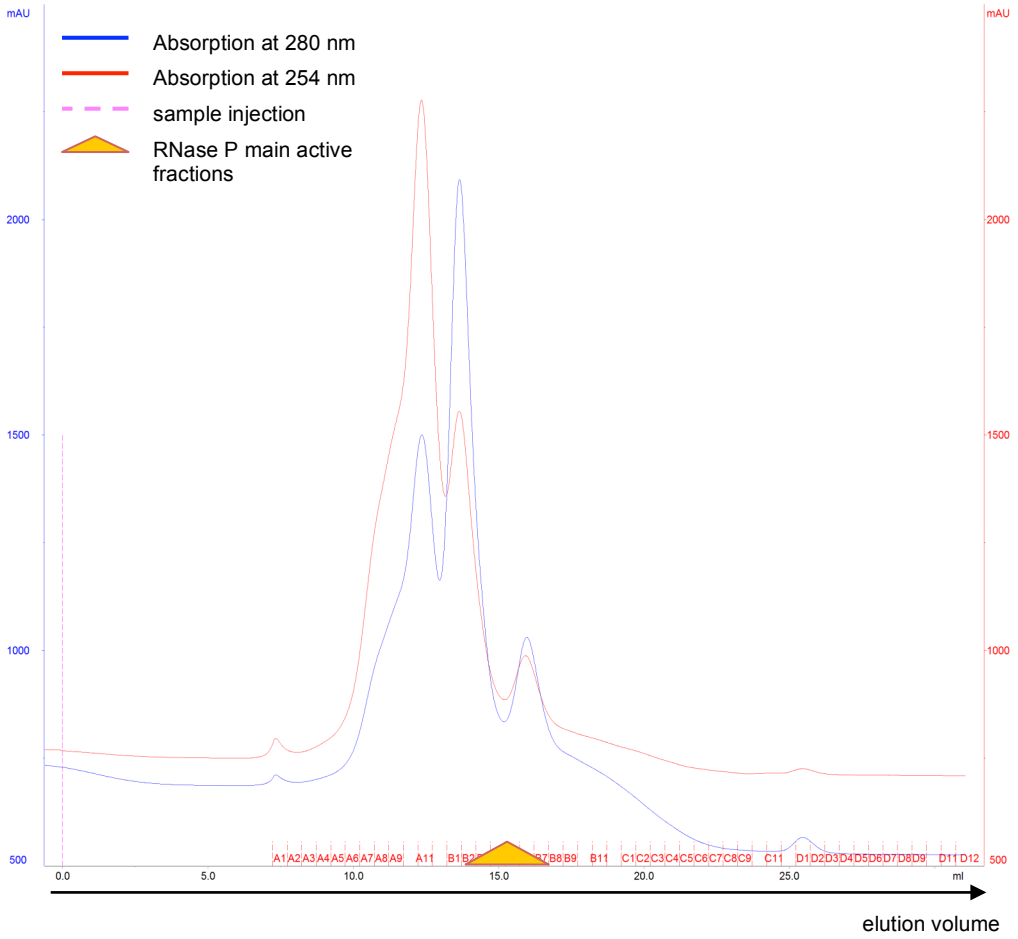

Figure S5: Chromatogram of the Superose 6 (SEC) column upon loading of a $HIC_{0.2}$ fraction. Fractions containing the bulk of RNase P activity reproducibly eluted after the major absorption peaks (elution buffer: A60), coinciding with a minimum in the UV absorption profile. The elution volume suggested a mass of approximately 350 kDa.

$SEC_{0.4}$ chromatogram

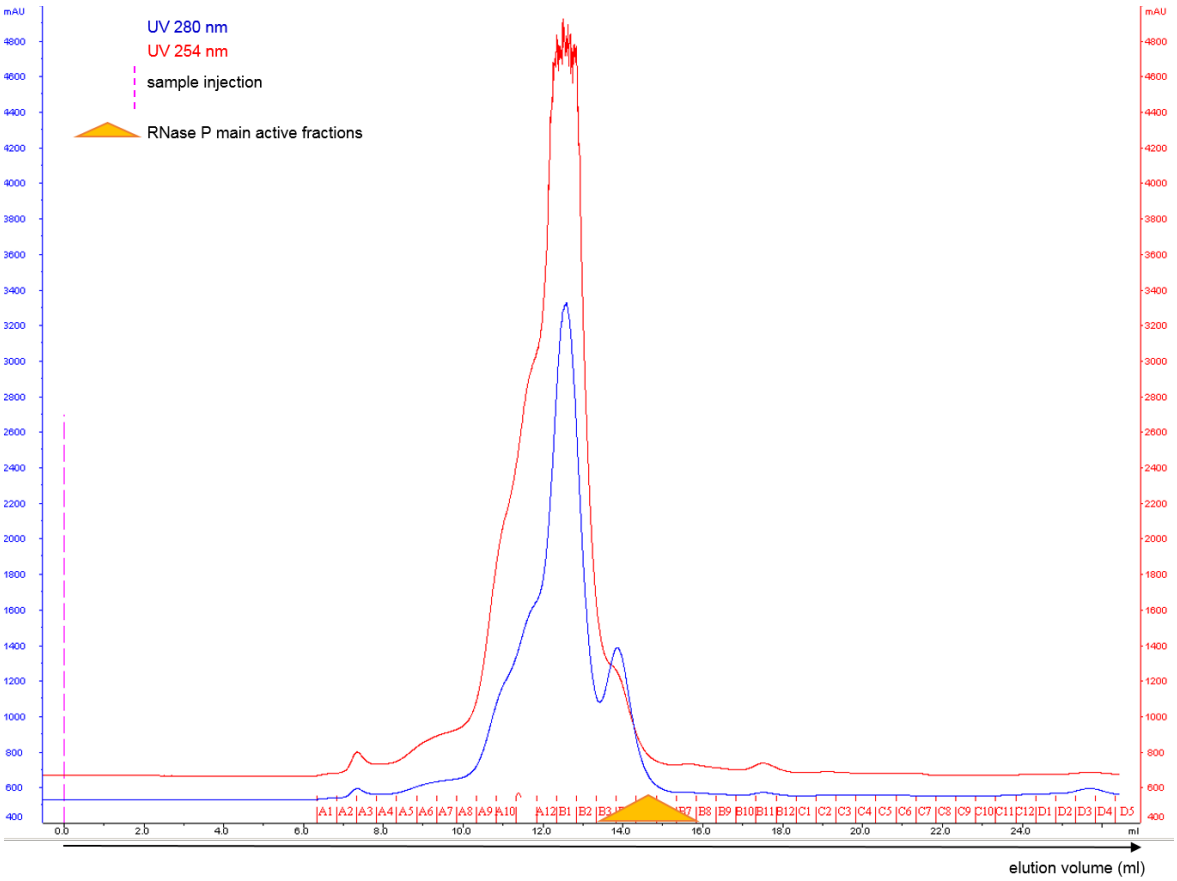

Figure S6: Chromatogram of the Superose 6 (SEC) column upon loading of a $HIC_{0.4}$ fraction. Fractions containing the bulk of RNase P activity coeluted with the descending shoulder of the second smaller peak (elution buffer: A260). The elution volume of fractions containing the bulk of RNase P activity suggested a mass of approximately 350 kDa.

Analysis of partially purified SEC fractions

After SEC chromatography of $HIC_{0.2}$ samples, the eluted "$SEC_{0.2}$" fractions were tested for RNase P activity and analyzed by 20% denaturing PAGE (Fig. S7). Several elution fractions were selected for further analysis by step gradient SDS-PAGE (Fig. 1B) of the main manuscript), representing the different regions of the RNase P activity peak: (I) fractions with no or weak RNase P activity [A10-A11], (II) fractions with increasing activity [A12, B1, B2], (III) one of the fractions with maximum activity [B4], (IV) fractions with gradually decreasing RNase P activity [B6, B8, B10] and (V) a fraction with low activity [B12].

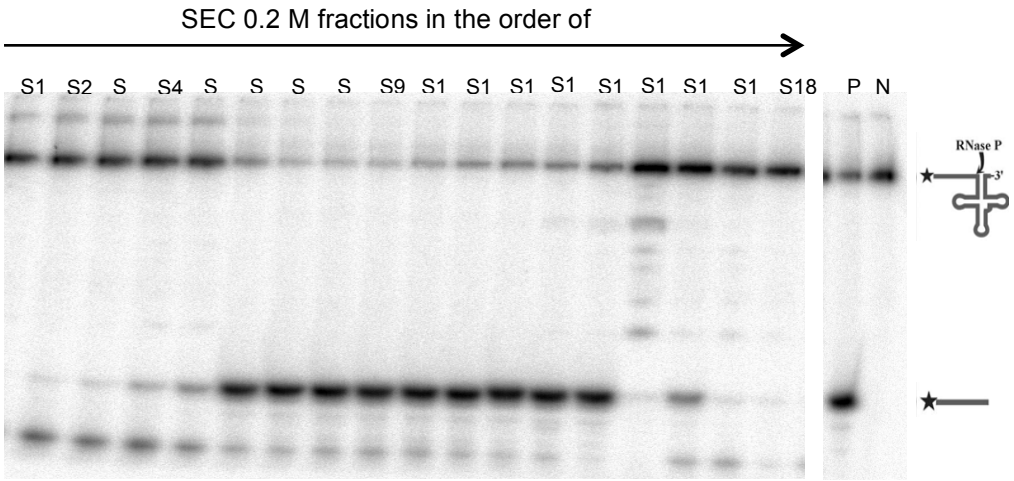

Figure S7. $SEC_{0.2}$ fractions covering the RNase P activity peak were tested for pre-tRNA processing; samples were analyzed by 20% denaturating PAGE. At the top of the gel, fractions are indicated in the order of elution from the Superose 6 column (S1 – S18); P: positive control, cleavage of pre-$tRNA^{Gly}$ by *E. coli* P RNA as in Fig. S2; N: negative control (ddH_2O instead of enzyme).

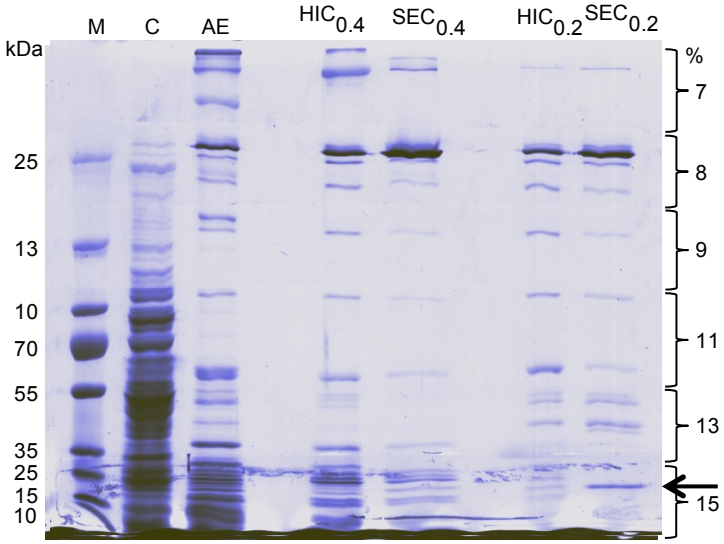

Figure S8. Protein pattern of RNase P active samples from each purification step. Samples of each purification step were analyzed by step gradient SDS-PAGE (SDS gel with several layers of different PAA concentrations). 2.5 µl of cell lysate (CL) were loaded in the second lane next to the protein marker (M; PageRuler Plus Prestained Protein Ladder, Thermo Scientific). "AEC" depicts 2.5 µl of a concentrated pool of RNase P activity fractions that eluted from the anion exchange column. The samples $HIC_{0.4}$ and $HIC_{0.2}$ (5 µl each) are the pooled, dialyzed and concentrated RNase P activity fractions that eluted in different HIC steps with elution buffer containing 0.4 M or 0.2 M $(NH_4)_2SO_4$. $SEC_{0.4}$ and $SEC_{0.2}$ are fractions (15 µl each) showing the highest RNase P activity after purification of the $HIC_{0.4}$ and $HIC_{0.2}$ samples by size exclusion chromatography. The protein pattern suggests that SEC purification and enrichment of RNase P acvtivity of $HIC_{0.2}$ samples was more efficient than SEC purification of $HIC_{0.4}$ samples, considering that the lower protein band (15 – 25 kDa) in the $SEC_{0.2}$ sample (arrow) was later identified as Aq_880 by Western Blot analysis. AEC: anion exchange chromatography; HIC: hydrophobic interaction chromatography; SEC: size exclusion chromatography.

Quantitative mass spectrometry (liquid samples with RNase P activity)

According to the results of the activity assays from RNase P-enriched $SEC_{0.2}$ and $SEC_{0.4}$ fractions, the elution fractions were classified as "-/+" (very low RNase P activity, increasing), "+" (increasing or decreasing activity), "++" (maximum activity) "+/-" (very low activity, decreasing). Fractions from each category were analyzed applying label-free quantitative mass spectrometry.

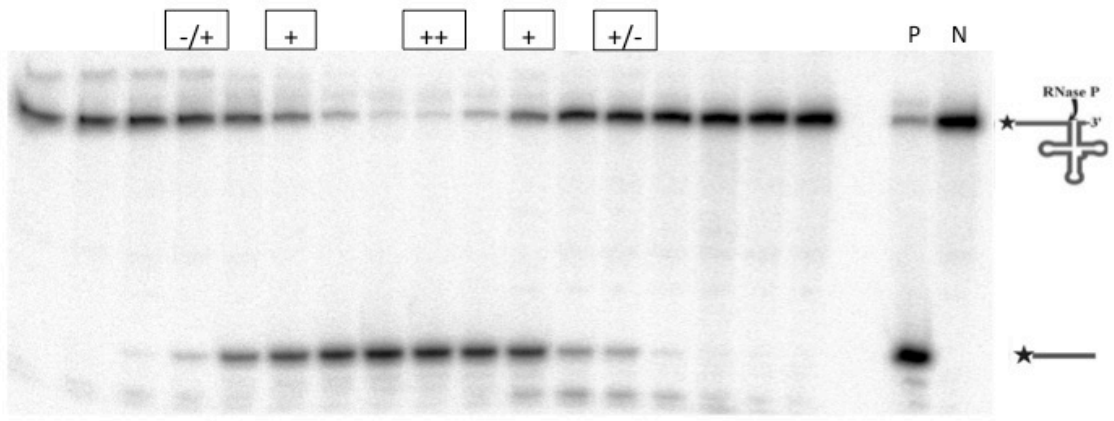

Figure S9. SEC fractions were tested for RNase P activity. Reaction products were analyzed by denaturating 20% PAGE in the order of elution from the Superose 6 column (here illustrated for $SEC_{0.4}$ fractions). "-/+": very low RNase P activity, increasing; "+": increasing or decreasing activity; "++": maximum activity; "+/-": very low RNase P activity, decreasing. P: positive control, cleavage of pre-$tRNA^{Gly}$ by *E. coli* P RNA as in Fig. S2; N: negative control (ddH_2O instead of enzyme).

The data obtained from quantitative mass spectrometry analysis were compared to the RNase P activity of the analyzed fractions. The *Peptide Spectrum Matches* value (∑PSM) was used as an indication for the quantitative amount of a certain protein in the analyzed fraction. The most abundant proteins in fractions containing maximum RNase P activity were (I) a hypothetical protein encoded by gene *aq_880*, (II) glutamine synthetase and (III) 30S ribosomal protein (r-protein) S2. Included in the analysis was a sample that was not SEC-purified following HIC purification. This sample contained the pooled and concentrated fractions that eluted during HIC in step 5 at 0 M $(NH_4)_2SO_4$ (= HIC_0). After concentration, RNase P activity was also detectable in these fractions. The sample HIC_0 was analyzed by mass spectrometry to search for common proteins also detectable in the $SEC_{0.2}$ and $SEC_{0.4}$ fractions displaying maximum RNase P activity (Fig. S10).

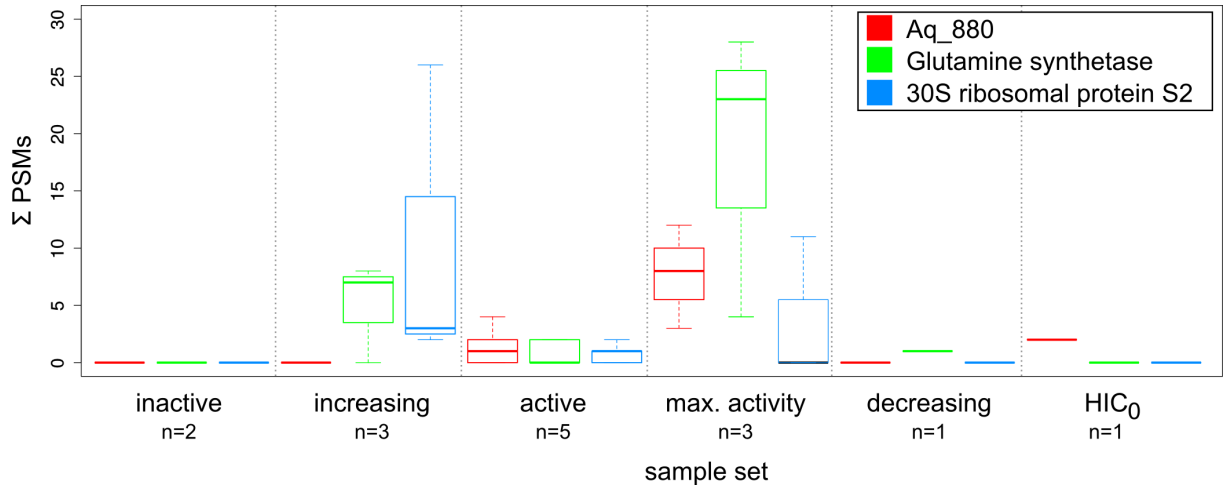

Figure S10. Boxplots for the three most abundant proteins in the fractions containing high RNase P activity (glutamine synthetase, Aq_880 and r-protein S2). The sum of *Peptide Spectrum Matches* (PSMs) for the specific protein is plotted over the height of RNase P activity of the analyzed SEC fraction according to Fig. S9 (inactive; -/+: low activity, increasing; +: active; ++: maximum (max.) activity; +/-: low activity, decreasing). Inactive: based on one $SEC_{0.2}$ and one $SEC_{0.4}$ sample (n = 2); increasing: based on two $SEC_{0.2}$ and one $SEC_{0.4}$ sample (n = 3); active: based on three $SEC_{0.2}$ and two $SEC_{0.4}$ samples (n = 5); max. activity: based on two $SEC_{0.2}$ and one $SEC_{0.4}$ sample (n = 3); decreasing: based on a single $SEC_{0.4}$ sample (n = 1); HIC_0 represented a single pool of concentrated fractions (with weak RNase P activity) that eluted in step 5 during HIC. Whiskers indicate the most extreme PSM sums found, boxes indicate the average range of 50% of all respective PSM sums in which the median of all values is shown as a thick line. For example, in the max. activity fraction, Aq_880 was found in three independent samples with PSM sums of 3, 8 and 12. Thus, the most extreme values are 3 and 12 (whiskers), while the average of all values (box) is in the range of 5.5 to 10 (means of 3 and 8, and 8 and 12) with a median of 8 (thick line).

As a result, only the protein Aq_880 was identified in both, the SEC fractions containing the highest RNase P activity and the concentrated HIC_0 fraction with moderate RNase P activity.

Apart from Aq_880, other abundant proteins were also identified in the SEC fractions containing maximum RNase P activity (in order of decreasing frequency): glutamine synthetase, the 30S ribosomal protein S2, the polynucleotide phosphorylase (PNPase), the N utilization substance protein B homolog (NusB) and Aq_707. Other ribosomal proteins were detected in fractions with increasing RNase P activity, but not in fractions with maximum activity. PNPase, NusB and Aq_707 were less abundant than Aq_880 and S2.

Excluding an *E. coli* RNase P RNA contamination in recombinant Aq_880 preparations

RT-PCR

RT-PCR analysis excluded a contamination with *E. coli* RNase P as the source of pre-tRNA processing by recombinant Aq_880 preparations (Fig. S11).

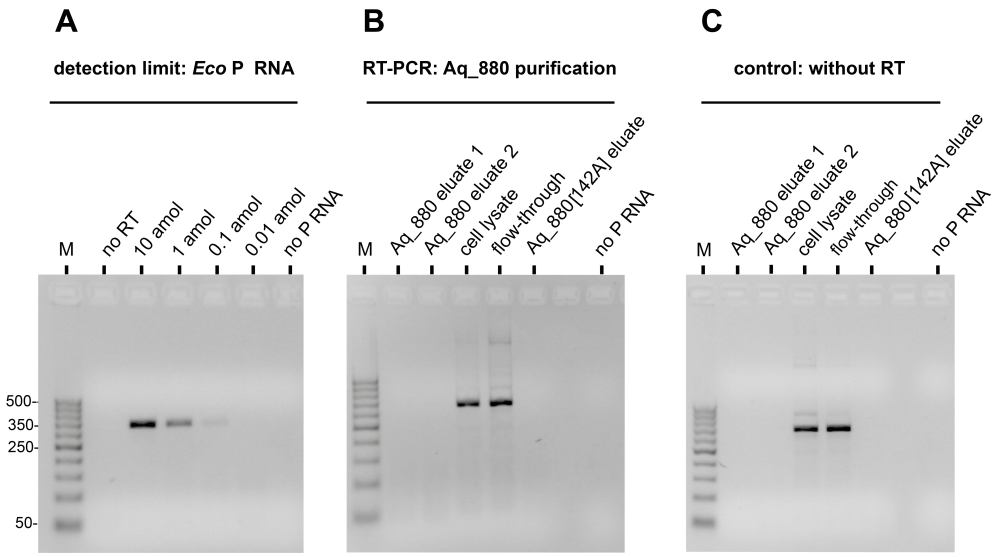

Figure S11: Detection of *E. coli* RNase P RNA (P RNA) by RT-PCR. All samples were extracted with phenol/chloroform and precipitated with ethanol before (RT-)PCR analysis. Three µl from each reaction were seperated on a 2% agarose gel and stained with ethidium bromide. **(A)** First, the detection limit of 0.1 amol (10^{-19} mol) P RNA was determined using a concentration range of 10 amol (10^{-17} mol) to 10 zmol (10^{-20} mol) of *in vitro*-transcribed *E. coli* P RNA. As a control, the RT-PCR reaction was performed in the absence of reverse transcriptase (no RT) or P RNA template (no P RNA) to exclude DNA contamination or unspecific amplification. M, 50-bp DNA ladder (Roth, Germany). **(B)** Ni-NTA-purified fractions of recombinant Aq_880 and Aq_880[D142A] were analyzed for the presence of *E. coli* P RNA by RT-PCR; 30 ng (1.25 pmol) batch-purified Aq_880 (Aq_880 eluate 1), FPLC-purified Aq_880 (Aq_880 eluate 2) or corresponding Aq_880[D142A] fractions were tested with primers specific for *E. coli* P RNA. As positive controls, 2.5 µl cell lysate (before loading onto the column) and 2.5 µl of the flow-through fraction were included. **(C)** In parallel, all fractions were tested for DNA contaminations in corresponding reactions but omitting reverse transcriptase. Bands in the cell lysate and flow-through indicate that DNA in these samples is also responsible for the signals in panel B.

Treatment with micrococcal nuclease (MN)

The conclusion that *A. aeolicus* RNase P Aq_880 is a protein-only enzymatic activity is corroborated by *in vitro* experiments with micrococcal nuclease (MN). The treatment with MN had no effect on the pre-tRNA processing activity of recombinant Aq_880. The same result

was seen in a parallel control experiment with PRORP1, the organellar protein-only RNase P from *Arabidopsis thaliana*. In contrast, incubation of *E. coli* P RNA or RNase P holoenzyme with MN completely abolished the pre-tRNA processing activity of this RNA-based enzyme. Unspecific binding of MN to pre-tRNA could make the cleavage site inaccessible for RNase P ("substrate masking", (46). Thus, a carrier RNA (*Bacillus subtilis* 6S-1 RNA) was added in 500-fold molar excess over pre-tRNA to processing assays to prevent unspecific binding of MN to pre-tRNA.

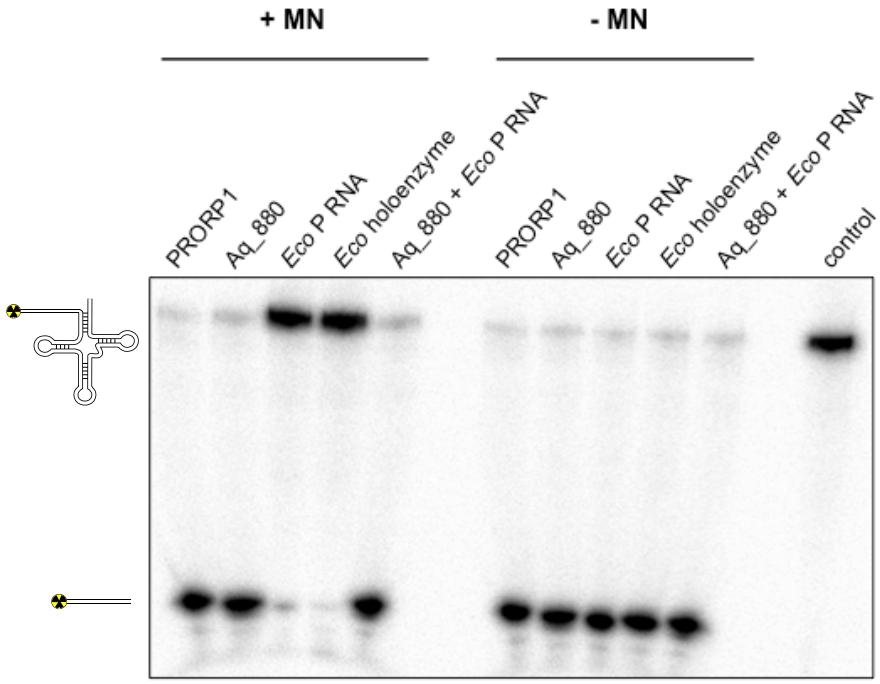

Figure S12. Processing of pre-tRNA^{Gly} by RNase P enzymes after treatment with micrococcal nuclease (MN). PRORP1: *A. thaliana* PRORP1; Aq_880: *A. aeolicus* Aq_880; *Eco* P RNA: *E. coli* RNase P RNA in the presence of 100 mM Mg^{2+}; *Eco* holoenzyme: *E. coli* RNase P holoenzyme in presence of 10 mM Mg^{2+}; Aq_880 + *Eco* P RNA: *A. aeolicus* Aq_880 plus *E. coli* P RNA; control: incubation of substrate in the absence of enzyme. + MN: RNase P samples pretreated with MN before pre-tRNA^{Gly} processing assays; - MN: as samples "+ MN", but omission of MN. For experimental details, see Supplementary Materials and Methods below.

Addition of recombinant Aq_707 / Aq_221 (PNPase) to *A. aeolicus* fractions with enriched RNase P activity

Since Aq_707 and Aq_221 (PNPase) copurified with RNase P activity and Aq_707 formed stable complexes with Aq_880 in SDS gels (band #6 in Fig. 1B of the main manuscript), we also tested if these recombinantly produced *A. aeolicus* proteins support RNase P activity. However, neither Aq_707 nor PNPase stimulated the RNase P activity of Aq_880. Not unexpected, PNPase caused some unspecific 3'-exonucleolytic degradation of the pre-tRNA and the 5'-leader cleavage product.

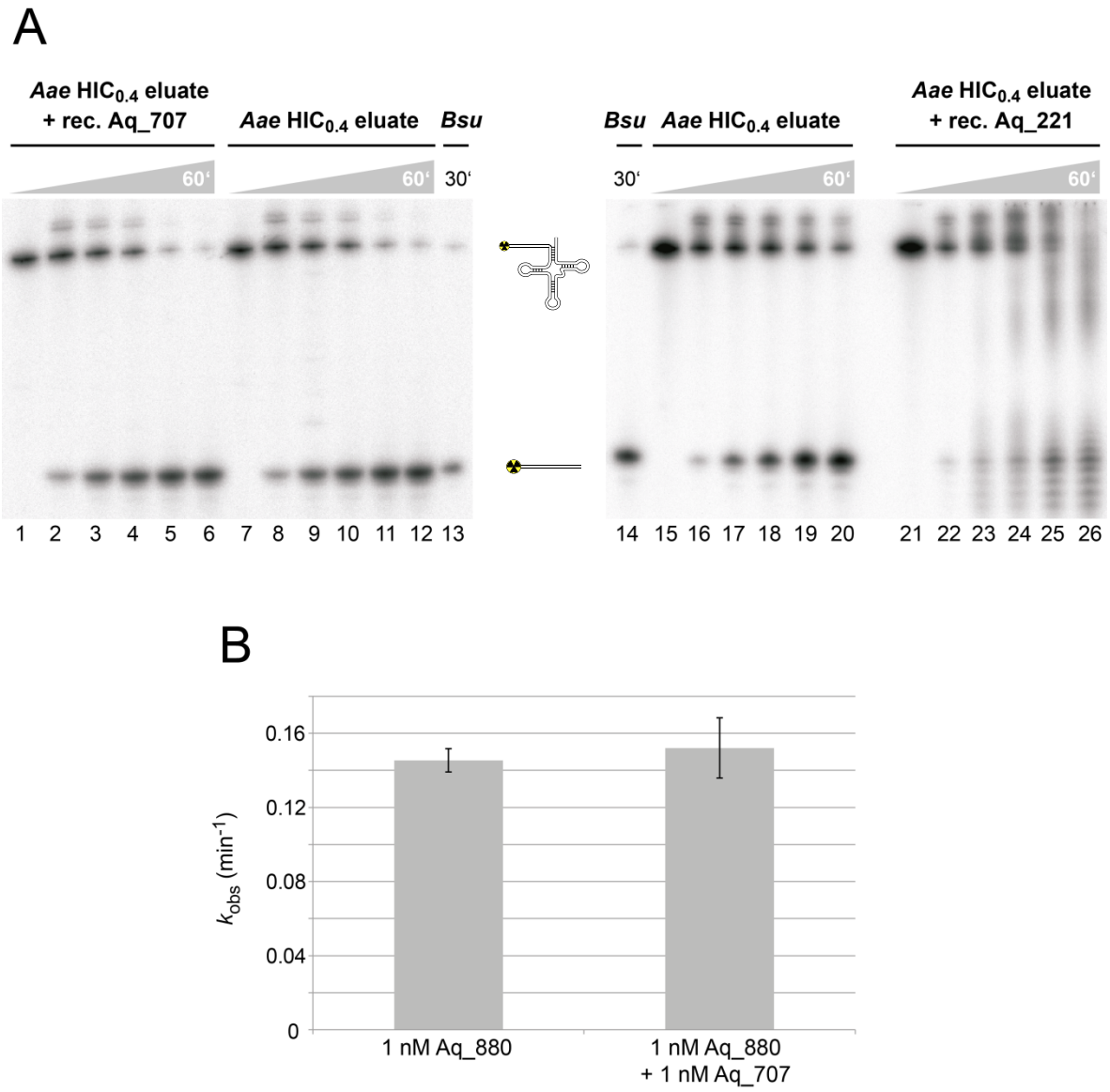

Figure S13. (**A**) Effect of recombinant *A. aeolicus* proteins Aq_707 or Aq_221 (PNPase) on RNase P activity of partially purified RNase P ($HIC_{0.4}$) fractions from *A. aeolicus*. Aliqouts were withdrawn after 1, 5, 10, 30 and 60 min. Lanes 1, 7, 15 and 21: pre-$tRNA^{Gly}$ incubated for 60 min in reaction buffer lacking the $HIC_{0.4}$ eluate and recombinant proteins was used as negative control (lanes 1, 7, 15, 21). *B*su: pre-$tRNA^{Gly}$ incubated for 30 min in the presence of 10 nM *B. subtilis* RNase P holoenzyme. For experimental details, see Suppl. Materials and Methods, "Cell lysate supplemented with recombinant proteins", p.37. (**B**) Cleavage of 5 nM pre-$tRNA^{Gly}$ by 1 nM recombinant Aq_880, either in the absence or presence of 1 nM Aq_707 in buffer F at 37°C; k_{obs} values are mean values derived from three independent experiments (single exponential decay based on time points at 0, 5, 15, 35 and 55 min), error bars are standard deviations of the mean. For further details, see Suppl. Materials and Methods, paragraph “Activity assay with recombinant Aq_880 variants”, p. 35.

Activity of recombinant Aq_880 in the presence of *A. aeolicus* total RNA

The preceding experiments provided no evidence for *A. aeolicus* RNase P activity depending on an essential RNA component. However, the possibility remained that RNA component(s) might support Aq_880 activity by exerting auxiliary structural or regulatory functions. Therefore, we analyzed Aq_880 activity under single-turnover conditions in the presence and absence of total *A. aeolicus* RNA either prepared as reported (8) (Method 1 without lysozyme) or as described in Suppl. Materials and Methods ("*A. aeolicus* total RNA preparation", acetic acid plus phenol/chloroform extraction). Such experiments (Fig. S14) showed that addition of *A. aeolicus* total RNA even had an inhibitory effect on the pre-tRNA processing activity of Aq_880. The relative rate constant k_{rel} is determined as the ratio of rate constants for Aq_880 with and without supplementation of total RNA ($k_{rel} = k_{obs(+RNA)} / k_{obs(-RNA)}$); k_{rel} was 0.47 at 37°C and 0.23 at 70°C assay temperature (mean value of two independent experiments each).

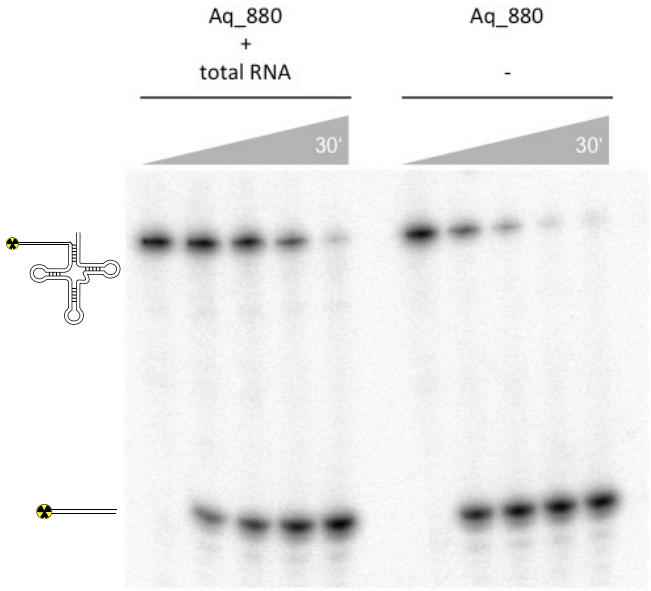

Figure S14. RNase P activity of Aq_880 (50 nM) in the presence and absence of *A. aeolicus* total RNA (20 ng/µl; prepared by acetic acid plus phenol/chloroform extraction) under single-turnover conditions at 37°C. Very similar results were obtained when procesing assays were performed at 70°C or with total *A. aeolicus* RNA prepared according to (8). For experimental details, see Suppl. Materials and Methods, paragraph "Aq_880 supplemented with total RNA", p. 37.

Thermostability of recombinant Aq_880

As the hyperthermophile *A. aeolicus* thrives at temperatures of up to 95°C, the thermostability of recombinant Aq_880 was determined in a cleavage assay using *in vitro*-transcribed pre-tRNA^{Gly} from the thermophilic bacterium *T. thermophilus*. In such assays, processing by recombinant Aq_880 was still observable at 70°C, but only residual activity was seen at 75°C and no activity at higher temperatures. The rate constant at 70°C (k_{obs} = 0.064 min^{-1}) was 15-fold lower than at 37°C (k_{obs} = 0.90 min^{-1}). As the rate decrease may have included contributions from increased dissociation rates of enzyme-substrate complexes and from denaturation of the pre-tRNA *in vitro* transcript lacking post-transcriptional nucleoside modifications that were shown to confer increased thermostability (37), we pursued a setup in which Aq_880 was preincubated for 10 min at 85°C before performing the pre-tRNA processing assay at 37°C. The k_{obs} slightly decreased from 1.17 min^{-1} (no preincubation at 85°C) to 0.79 min^{-1} with preincubation at 85°C (see Fig. 2F of the main manuscript). Thus, the preincubation step decreased the enzymatic activity by not more than ~30%, consistent with thermostability of Aq_880. Applying the same heat treatment to the *E. coli* RNase P holoenzyme essentially resulted in a complete loss of its enzymatic activity (k_{obs} = 0.005 min^{-1}) compared to preincubation at 37°C (k_{obs} = 1.37 min^{-1}). The same kind of analysis was performed with a native $HIC_{0.4}$ fraction (see Fig. S3), giving very similar results (see Fig. 2F of the main manuscript).

Oligomerization of recombinant Aq_880

The elution volume of recombinant Aq_880 on a calibrated Superose 6 column corresponded to a mass of approximately 420 kDa (Fig. S15). The protein eluted closely after apoferritin (443 kDa) that was used for column calibration. The result agrees with the estimates of about 350 kDa based on the elution volume of partially purified SEC fractions with maximum RNase P activity during the third purification step (Superose 6 column, Fig. S5 to S7).

SDS-PAGE analysis of the fractions eluting from the Superose 6 column loaded with recombinant Aq_880 (Fig. S15) revealed weak protein bands at about 50 and 70 kDa in the fractions with the highest concentration of Aq_880 (Fig. S16, arrows). In the minor band at around 70 kDa, exclusively *A. aeolicus* Aq_880 was identified by mass spectrometry. This correlates with the size of the extra band in the Aq_880 Western blot (Fig. 3B of the main manuscript; migrating there somewhat faster because of lack of the His tag). The band migrating at ~ 50 kDa was identified as the *E. coli* maltoporin precursor. This indicates that Aq_880 forms stable trimers that are able to persist during SDS-PAGE. Considering that the major elution peak of Aq_880 corresponded to a mass of approximately 420 kDa, it is possible that Aq_880 occurs in oligomeric forms consisting of 3 hexamers or 6 trimers.

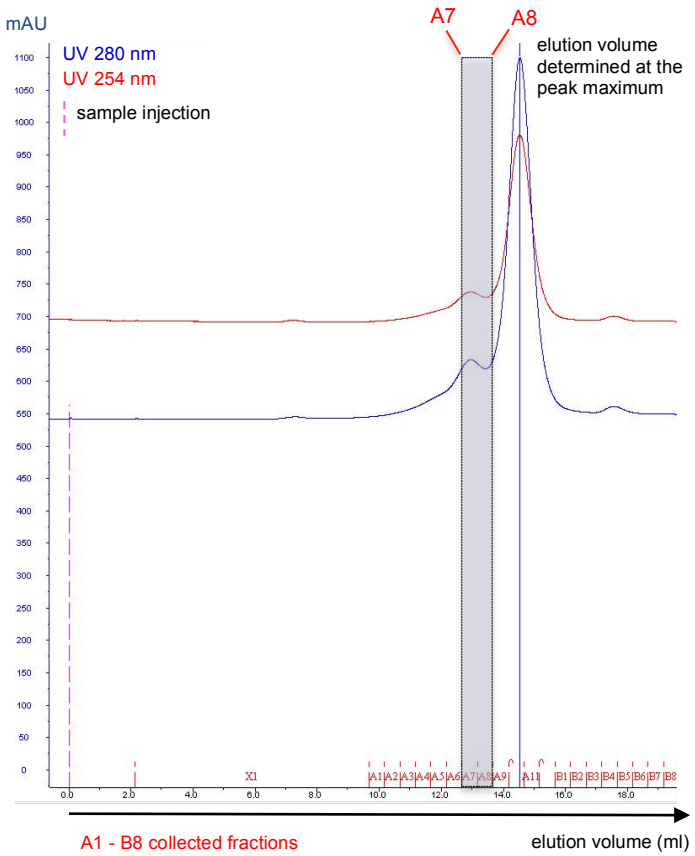

Figure S15. Elution profile of recombinant Aq_880 in buffer S (50 mM Tris-HCl pH 7.45, 150 mM NaCl, 4.5 mM $Mg(OAc)_2$, 5 mM DTT,) on a Superose 6 column (flow rate: 0.3 ml/min). The elution volume was determined at the peak maximum. Fractions of 0.5 ml were collected and analyzed by SDS-PAGE. The fractions collected from the small peak preceding the main peak were analyzed as well (fractions A7 and A8).

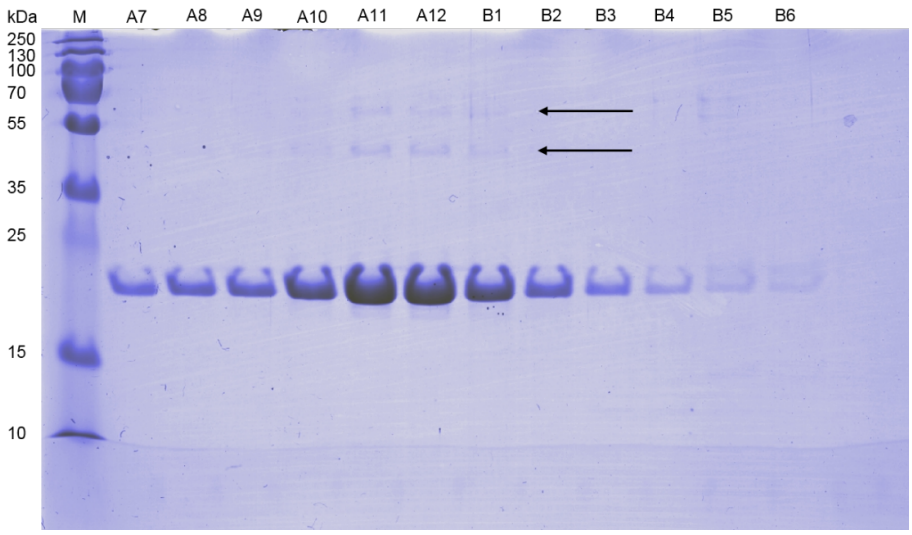

Figure S16. SDS-PAGE analysis of fractions A7 – B6 eluting form the Superose 6 column loaded with recombinant C-terminally His-tagged Aq_880 (FPLC-purified). Protein bands were detected by sensitive colloidal Coomassie staining. The corresponding chromatogram is shown in Fig. S15. The arrows point to the additional weak signals at about 50 and 70 kDa that became visible in the peak fractions A10-B1. Only a single band of the size of monomeric Aq_880 (23.7 kDa, with C-terminal His tag) was detectable in fractions A7 and A8 that were collected from the small peak preceding the main peak. 15% SDS-PAGE; M: Protein marker.

Identification of active site residues in Aq_880

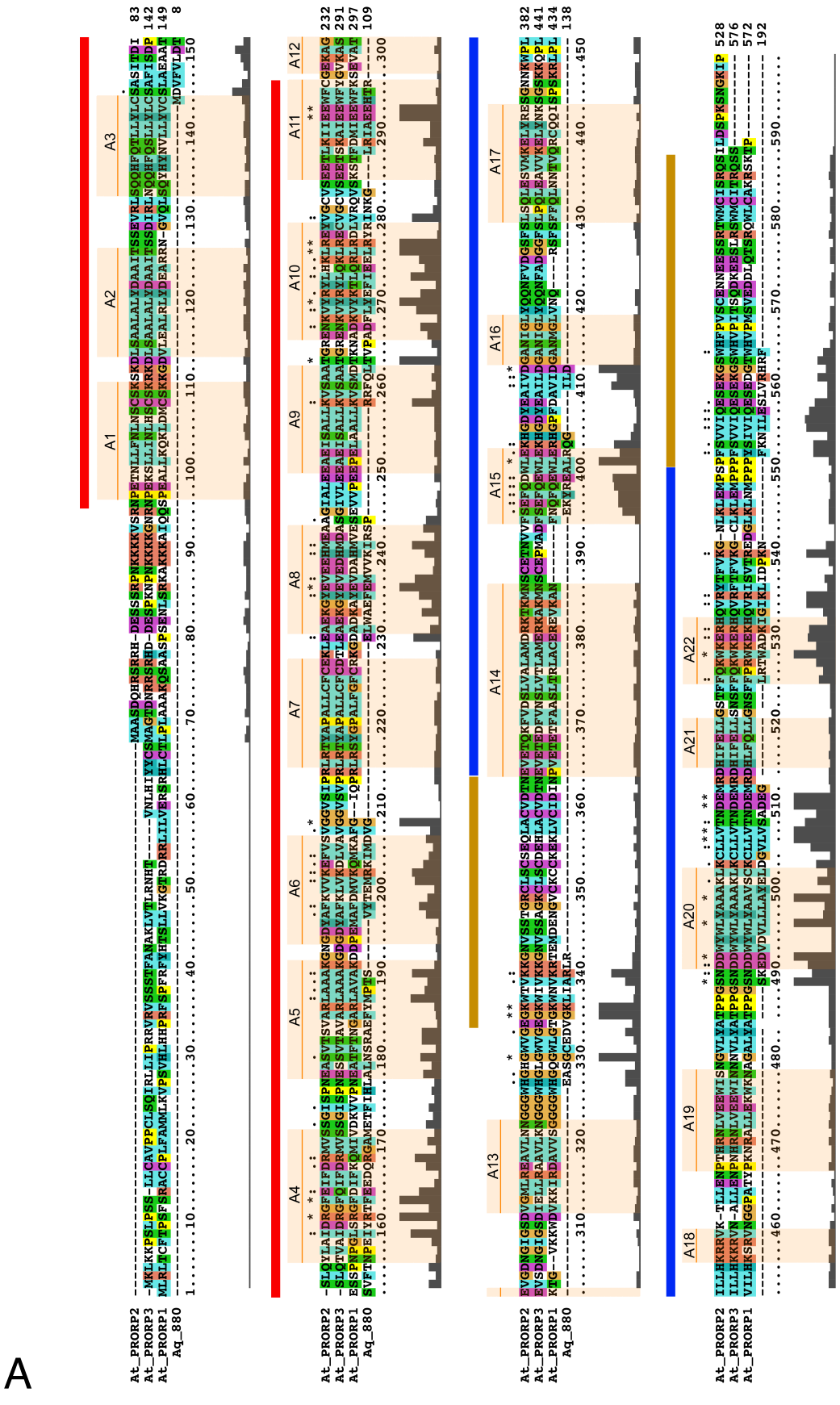

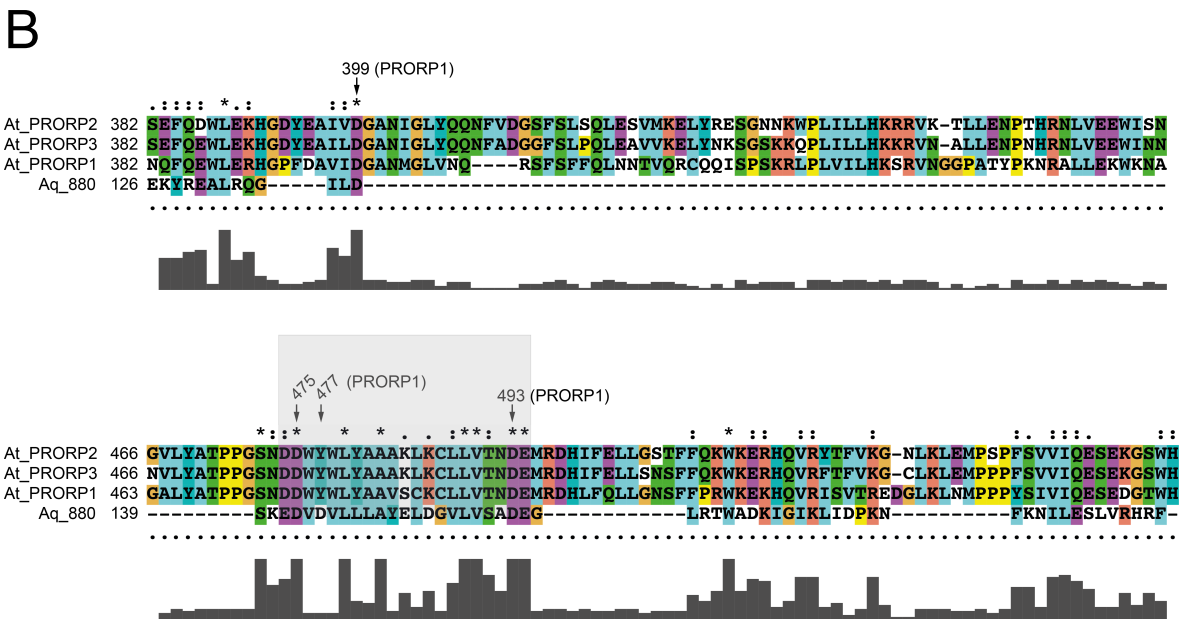

Figure S17. (**A**) Clustal Omega (38) alignment of full-length *A. thaliana* PRORP1-3 (At_PRORP1-3) and Aq_880. The α-helical elements inferred from the X-ray structure of At_PRORP1 (21) are numbered A1–A22 above the sequences. The amino acid positions of the pentatricopeptide repeat domain (red boxes at the top, residues 95-292 of At_PRORP1), the central domain (golden boxes, residues 328-357 and 534-570 of At_PRORP1) and the metallonuclease domain (blue boxes at the top, residues 358-533 of At_PRORP1) are indicated. (**B**) Section of the alignment that revealed similarities of Aq_880 to *A. thaliana* PRORP1-3 in their metallonuclease domains (Nedd4-BP1, YacP nucleases = NYN domains); in the area highlighted in gray, candidates for catalytic aspartates of Aq_880 were identified. In addition, D138 of Aq_880 was considered as a catalytic aspartate corresponding to D399 of At_PRORP1.

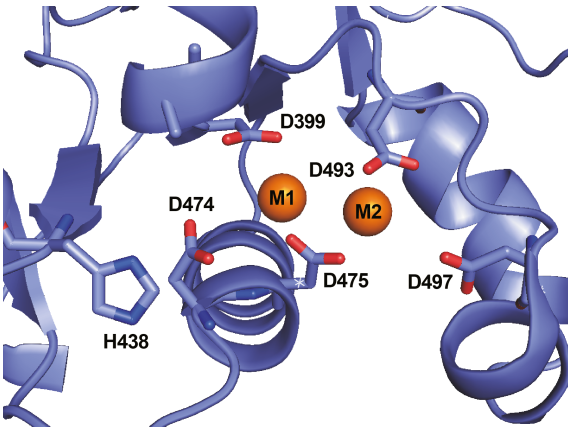

Figure S18. Illustration of the catalytic metal ion binding sites in *A. thaliana* PRORP1. Based on the alignment of PRORP enzymes and Aq_880 (Fig. S17), Aq_880 residues D138, D142 and D160 were inferred to correspond to D399, D475 and D493 of PRORP1. The aspartic acid residue chains in the active center of PRORP1 are shown as sticks. The side chains of D399, D474, D475 and D493 are supposed to coordinate two catalytic metal ions (orange spheres). The illustration is based on the *A. thaliana* PRORP1 crystal structure (21).

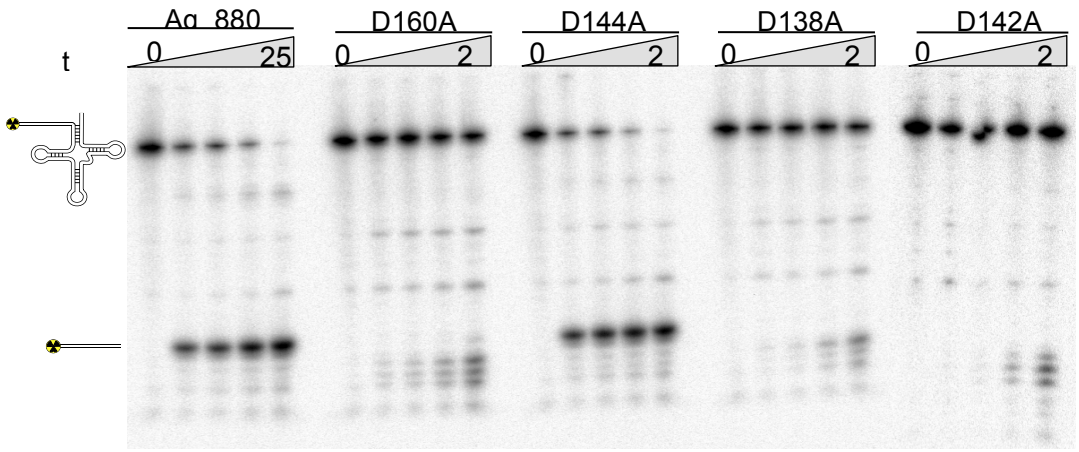

Figure S19. *In vitro* pre-tRNA processing assay under single-turnover conditions (50 nM enzyme, < 1nM substrate) to investigate the function of Aq_880 variants with mutation of aspartic acid residues (to alanine) potentially involved in catalysis. All proteins carried a C-terminal His tag; assays were performed at 37°C. The pre-tRNA^{Gly} (upper band) was 5'-[^{32}P]-endlabeled. Mutants D160A, D138A and D142A were inactive, only mutant D144A was similarly active as wild-type Aq_880.

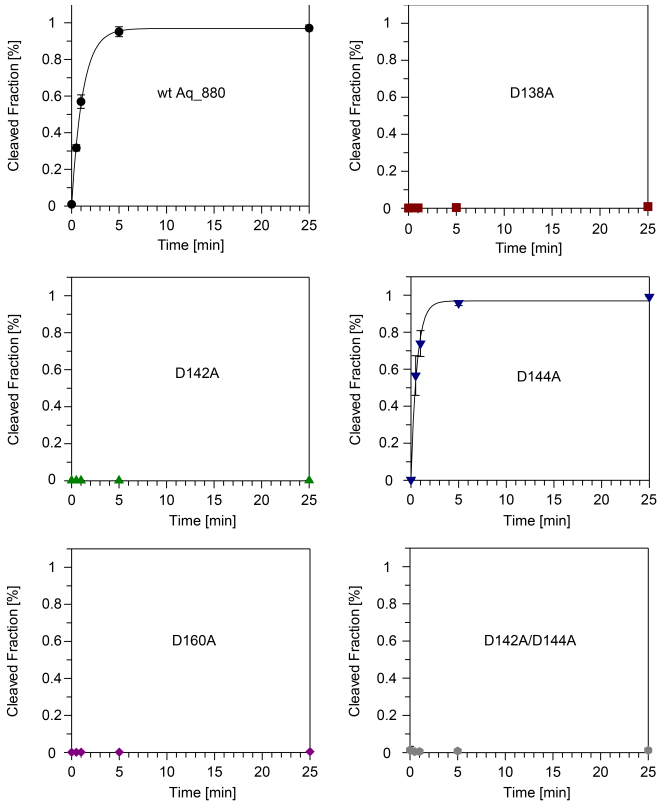

Figure S20. Graphical illustration of *in vitro* pre-tRNA^{Gly} processing assays of the type presented in Fig. S19. The fraction of processed pre-tRNA was plotted against the time [min]. The values are mean values of three independent single-turnover experiments performed at 37°C. Essentially no activity was detectable for the mutants D138A, D142A, D160A and D142A/D144A. For wild-type Aq_880 and the mutant D144A enzyme, we calculated k_{obs} values of 0.93 ± 0.05 min^{-1} and 1.6 ± 0.13 min^{-1} under these test conditions.

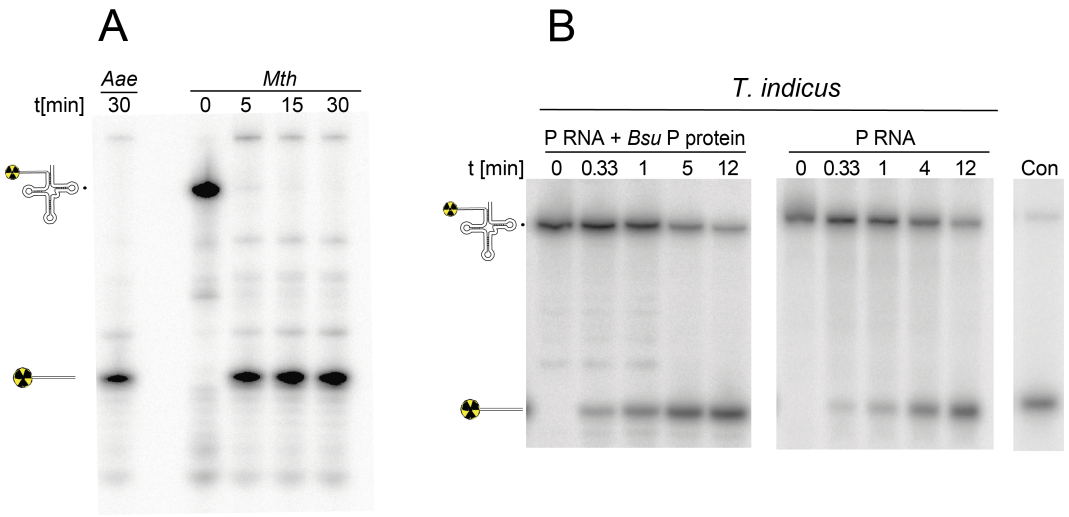

Figure S21. Activity assays for RNA-based and HARP RNase P from *Thermodesulfatator indicus* (bacterium) and HARP from *Methanothermobacter thermautrophicus* Delta H (archaeon). (**A**) Enzymatic activity of archaeal HARP from *M. thermautotrophicus* (*Mth*) was analyzed as described in the Suppl. Materials and Methods, paragraph "Activity assays using other HARP proteins" (p. 38). Samples were separated by 20% denaturing PAGE. A corresponding assay with Aq_880 (*Aae*, 30 min of incubation) served as control (see Suppl. Materials and Methods, paragraph "Activity assay with recombinant Aq_880 variants", p. 35). (**B**) Enzymatic activity of the chimeric holoenzyme composed of *T. indicus* P RNA and *B. subtilis* P protein and *T. indicus* P RNA alone was analyzed as described in Suppl. Materials and Methods, paragraph, "Activity assays with other bacterial RNase P RNAs" (p. 38). As control (lane Con), an RNase P holoenzyme consisting of *E. coli* P RNA and *B. subtilis* P protein was reconstituted as described for the chimeric *T. indicus* enzyme and incubated with the substrate for 12 min before gel loading. RNA-based RNase P of *M. thermautotrophicus* was not tested *in vitro* as the enzyme was previously characterized in much detail (3) (15) (16).

Bioinformatic analysis

Evaluation of proteins identified in quantitative and qualitative mass spectrometry analyses

Of all proteins identified in the quantitative and qualitative mass spectrometry analyses, the hypothetical protein Aq_880 appeared as the most promising one, because it was the most abundant candidate and it was the only protein that was detected in both, $SEC_{0.2}$/$SEC_{0.4}$ fractions with maximum RNase P activity and in the minor HIC_0 fractions with weak RNase P activity (Fig. S10). The structure prediction of Aq_880 revealed similarities to a solution structure of an endonuclease and showed similarity to a PIN (PilT N-terminal) domain. Since PIN domains function as ribonucleases (2) and the catalytic metallonuclease domain of the protein-only RNase P (PRORP) belongs to the PIN domain-like fold superfamily (44), the Aq_880 protein was considered to function as an RNase P in *A. aeolicus*. The importance of the hypothetical protein Aq_880 is underlined by its exclusive appearance in the *Aquificaceae* branch lacking any bacterial-like RNase P (25) (27) (Fig. S22).

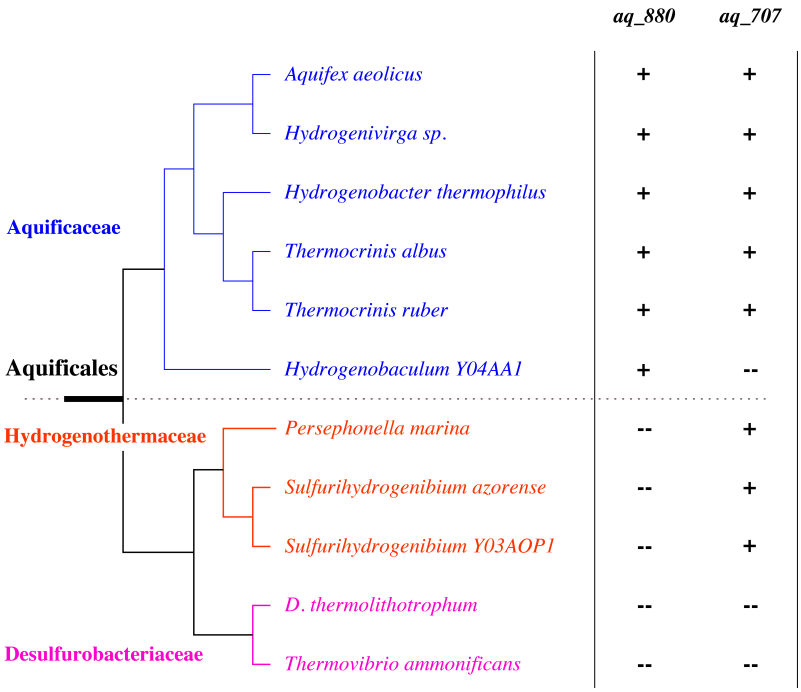

Figure S22. Identification of *aq_880* and *aq_707* homologs within the *Aquificales*. The search was performed with tblastn applying an *e* value threshold of 10^{-5}. The phylogenetic tree was adapted from (25). Aq_707 was included in the analysis because (i) the protein copurified with RNase P activity, (ii) Aq_707 formed stable complexes with Aq_880 (see main manuscript), and (iii) the protein was predicted as a tRNA methyltransferase homolog (see text below).

Analysis of structural domains

The most abundant proteins in the SEC fractions with maximum RNase P activity were further analyzed by structural bioinformatics using PHYRE2 in the intensive mode (22). As we were searching for *A. aeolicus* RNase P, the focus was put on RNA-binding properties and endonucleolytic function. The alignment and structure prediction of Aq_880 showed similarities to the PIN (PilT N-terminal) domain that belongs to the PIN domain-like superfamily. The metallonuclease domain of the protein-only RNase P (PRORP1) contains a NYN (N4BP1, YacP-like Nuclease) domain (1) (21) which also belongs to the PIN domain-like superfamily. The identity value between Aq_880 and the PIN domain was only 28% but the confidence of the result was 97.5%. The relatively low identity might be attributable to only part of the PIN domain protein serving as template for the alignment with Aq_880 that essentially is a PIN domain only. The alignment resulted in additional hits for RNA binding (functionally unknown protein from *Methanocaldococcus jannaschii*, 21% identity, 98.5% confidence) and metal binding (endonuclease Nob1 from *Pyrococcus horikoshii*, 33% identity, 98.9% confidence) proteins. Regarding the fact that all RNase P enzymes identified up to date are metalloendonucleases, Aq_880 became a top candidate for an *A. aeolicus* RNase P component. The analysis of the *A. aeolicus* PNPase pointed to a structural similarity between the PNPase and bacterial P proteins. (41) already analyzed the structure

of the PNPase from *Streptomyces antibioticus* and described bacterial RNase P proteins as likely structural homologs of PNPase/GPSI domains. According to the SCOP (29) and the SUPERFAMILY database (12), PNPase/GPSI domains are a member of the *Ribonuclease PH domain 1-like* family, which, together with the *RNase P protein* family, belong to the *Ribosomal protein S5 domain 2-like* superfamily. As PNPase is known to be an exonuclease we followed this track with regard to structural similarity. The analysis of the hypothetical protein Aq_707 revealed partial similarities (20 – 22%, confidence: 100%) with MnmC proteins from *E. coli* and *Yersinia pestis* that are involved in tRNA 5-methylaminomethyl-2-thiouridine biosynthesis. In *E. coli*, MnmC is a bifunctional tRNA modification enzyme with methyltransferase activity. Since one subunit (TRMT10C) of the human mitochondrial RNase P is a methyltransferase (20), (44), the hypothetical protein Aq_707 moved into our focus despite the fact that the methyltransferase homolog has already been identified in *A. aeolicus* (23). Nonetheless, Aq_707 remained in our focus based on its potential to be a protein that acts on tRNAs.

Furthermore, we analyzed the glutamine synthetase. Although the structure and function of this enzyme is known, we performed structure predictions and alignments, taking into consideration that *A. aeolicus* glutamine synthetase might have acquired additional, yet unknown, functions during evolution. However, the results neither provided support in favor of such a possibility nor did we find any evidence for an RNA binding domain. Regarding NusB, which plays an important role in transcriptional antitermination, its RNA-binding properties and sites are known (9) (39). Its structure analysis failed to give any hints on additional functions that might be related to RNase P activity.

Occurrence of protein candidates within the *Aquificales* and alignment of bacterial and archaeal Aq_880 homologs

Despite intensive bioinformatic efforts neither a gene for a bacterial-type RNase P protein subunit nor an RNA subunit could be identified in *A. aeolicus* or any other member of the

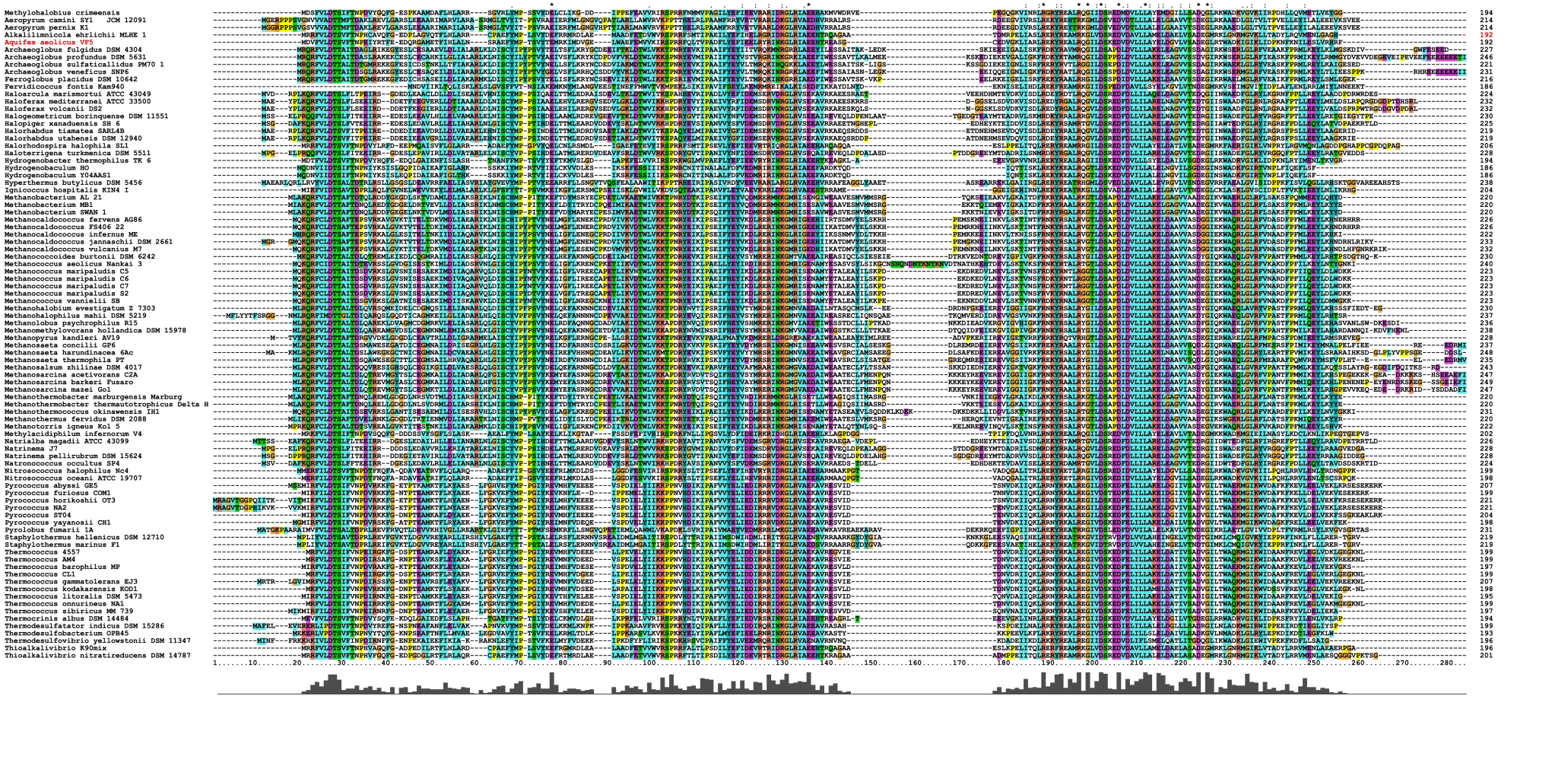

Figure S23. Clustal Omega multiple sequence alignment of Aq_880 homologs among Bacteria and Archaea. For details, see Supplementary Materials and Methods.

family of the *Aquificaceae*. However, bacterial-type RNase P enzymes have been identified in other *Aquificales*, including all species that belong to the families *Desulfurobacteriaceae* and *Hydrogenothermaceae* which, together with the *Aquificaceae*, form the order *Aquificales* (25) (26). We thus assumed that the RNase P from *Aquificaceae* differs from the RNase P of *Desulfurobacteriaceae* and *Hydrogenothermaceae.* Therefore, the proteins identified in RNase P-enriched *A. aeolicus* fractions were analyzed for commonalities among *Aquificaceae* and concomitant differences to homologs from the *Desulfurobacteriaceae* and *Hydrogenothermaceae*. Yet, most informative was the presence or absence of proteins in the three families belonging to the *Aquificales* (Fig. S22). The glutamine synthetase, NusB, PNPase and ribosomal protein S2 were found to be represented in all three families, which was expected for housekeeping genes. The hypothetical protein encoded by gene *aq_707* was not detected in the *Desulfurobacteriaceae* and in the species *Hydrogenobaculum sp. Y04AAS1* (Fig. S22), which belongs to the *Aquificaceae*, but was identifiable in the *Hydrogenothermaceae* expressing canonical bacterial RNase P enzymes (26). In contrast, as mentioned above, aq_880 homologs were exclusively found in all analyzed members of the *Aquificaceae*, but not in any of the two other families of the *Aquificales*.

Aq_880 homologs were identified in many Archaea and a small group of bacteria beyond the *Aquificaceae* (Fig. S23, S24 and Table S1). For more information, see the main manuscript.

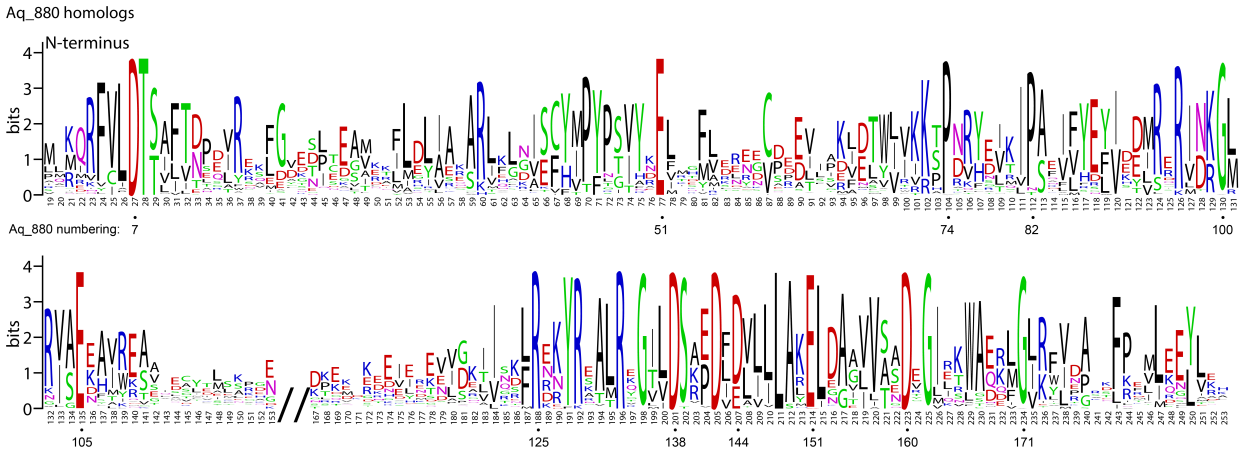

Figure S24. WebLogo to illustrate amino acid conservation among the Aq_880 homologs aligned in Fig. S23. In addition to the numbering based on the alignment of Fig. S23, residue numbers in Aq_880 are indicated for some of the conserved amino acids. For more details, see Suppl. Materials and Methods.

Species	HARP	RNA	RnpA	Rpp29	Pop5	Rpp30
Bacteria						
Aquificae -> Aquificae -> *Aquificales* -> *Aquificaceae*						
Aquifex aeolicus VF5	yes				yes	yes
Hydrogenobacter thermophilus TK 6	yes				yes	yes
Hydrogenobaculum HO	yes				yes	yes
Hydrogenobaculum SN	yes				yes	yes
Hydrogenobaculum Y04AAS1	yes				yes	yes
Thermocrinis albus DSM 14484	yes				yes	yes
Proteobacteria -> Gammaproteobacteria -> *Chromatiales* → *Chromatiaceae*						
Nitrosococcus halophilus Nc4	yes	yes	yes		(yes)	yes
Nitrosococcus oceani ATCC 19707	yes	yes	yes		(yes)	
Proteobacteria -> Gammaproteobacteria -> *Chromatiales* -> *Ectothiorhodospiraceae*						
Alkalilimnicola ehrlichii MLHE 1	yes	yes	yes		(yes)	
Halorhodospira halophila SL1	yes	yes	yes			
Thioalkalivibrio K90mix	yes	yes	yes		yes	
Thioalkalivibrio nitratireducens DSM 14787	yes	yes	yes		yes	
Proteobacteria -> Gammaproteobacteria -> Methylococcales						
Methylohalobius crimeensis	yes	yes	yes			yes
Verrucomicrobia -> *Methylacidiphilales* -> *Methylacidiphilaceae*						
Methylacidiphilum infernorum V4	yes	yes	yes		(yes)	yes
Thermodesulfobacteria -> Thermodesulfobacteria -> *Thermodesulfobacteriales* -> *Thermodesulfobacteriaceae*						
Thermodesulfatator indicus DSM 15286	yes	yes	yes			yes
Thermodesulfobacterium geofontis OPF15 (initially termed *Thermodesulfobacterium* OPB45)	yes	yes	yes			yes
Nitrospirae -> Nitrospira -> *Nitrospirales* -> *Nitrospiraceae*						
Thermodesulfovibrio yellowstonii DSM 11347	yes					yes
Archaea						
Thermococci -> *Thermococcales* -> *Thermococcaceae*						
Pyrococcus NA2	yes	yes		yes	yes	yes
Pyrococcus ST04	yes	yes		(yes)	yes	yes
Pyrococcus abyssi GE5	yes	yes		yes	yes	yes
Pyrococcus furiosus COM1	yes	yes		yes	yes	yes
Pyrococcus furiosus DSM 3638	yes	yes		yes	yes	yes
Pyrococcus horikoshii OT3	yes	yes		yes	yes	yes
Pyrococcus yayanosii CH1	yes	yes		yes	yes	yes
Thermococcus 4557	yes	yes		yes	yes	yes
Thermococcus AM4	yes	yes		yes	yes	yes
Thermococcus CL1	yes	yes		(yes)	yes	yes

Thermococcus barophilus MP	yes	yes	yes	yes	yes
Thermococcus gammatolerans EJ3	yes	yes	yes	yes	yes
Thermococcus kodakarensis KOD1	yes	yes	yes	yes	yes
Thermococcus litoralis DSM 5473	yes	yes	yes	yes	yes
Thermococcus onnurineus NA1	yes	yes	yes	yes	yes
Thermococcus sibiricus MM 739	yes	yes	yes	yes	yes
Halobacteria -> *Halobacteriales* -> *Halobacteriaceae*					
Haloarcula marismortui ATCC 43049	yes	yes	(yes)	yes	yes
Halorhabdus tiamatea SARL4B	yes	yes	yes	yes	yes
Halorhabdus utahensis DSM 12940	yes	yes	yes	yes	yes
Halobacteria -> *Haloferacales* -> *Haloferacaceae*					
Haloferax mediterranei ATCC 33500	yes	yes	yes	yes	yes
Haloferax volcanii DS2	yes	yes	yes	yes	yes
Halogeometricum borinquense DSM 11551	yes*	yes	(yes)	(yes)*	(yes)
Halobacteria -> *Natrialbales* -> *Natrialbaceae*					
Halopiger xanaduensis SH 6	yes	yes	yes	yes	yes
Haloterrigena turkmenica DSM 5511	yes	yes	yes	yes	yes
Natrialba magadii ATCC 43099	yes	yes	yes	yes	yes
Natrinema J7	yes	yes	yes	yes	yes
Natrinema pellirubrum DSM 15624	yes	yes	yes	yes	yes
Natronococcus occultus SP4	yes	yes	yes	yes	yes
Archaeoglobi -> *Archaeoglobales* -> *Archaeoglobaceae*					
Archaeoglobus fulgidus DSM 4304	yes	yes	yes	yes	yes
Archaeoglobus profundus DSM 5631	yes	yes	yes	yes	yes
Archaeoglobus sulfaticallidus PM70 1	yes	yes	yes	yes	yes
Archaeoglobus veneficus SNP6	yes	yes	yes	yes	yes
Ferroglobus placidus DSM 10642	yes	yes	yes	yes	yes
Methanobacteria -> *Methanobacteriales* -> *Methanobacteriaceae*					
Methanobacterium AL 21	yes	yes	yes	yes	yes
Methanobacterium MB1	yes	yes	yes	yes	yes
Methanobacterium SWAN 1	yes	yes	yes	yes	yes
Methanothermobacter marburgensis Marburg	yes	yes	yes	yes	yes
Methanothermobacter thermautotrophicus Delta H	yes	yes	yes	yes	yes
Methanobacteria -> *Methanobacteriales* -> *Methanothermaceae*					
Methanothermus fervidus DSM 2088	yes	yes	yes	yes	yes
Methanococci -> *Methanococcales* -> *Methanocaldococcaceae*					
Methanocaldococcus FS406 22	yes	yes	yes	yes	yes
Methanocaldococcus fervens AG86	yes	yes	yes	yes	yes

Methanocaldococcus infernus ME	yes	yes	yes	yes	yes
Methanocaldococcus jannaschii DSM 2661	yes	yes	yes	yes	yes
Methanocaldococcus vulcanius M7	yes	yes	yes	yes	yes
Methanotorris igneus Kol 5	yes	yes	yes	yes	yes
Methanococci -> *Methanococcales* -> *Methanococcaceae*					
Methanococcus aeolicus Nankai 3	yes	yes	yes	yes	yes
Methanococcus maripaludis C5	yes	yes	yes	yes	yes
Methanococcus maripaludis C6	yes	yes	yes	yes	yes
Methanococcus maripaludis C7	yes	yes	yes	yes	yes
Methanococcus maripaludis S2	yes	yes	yes	yes	yes
Methanococcus maripaludis X1	yes	yes	yes	yes	yes
Methanococcus vannielii SB	yes	yes	yes	yes	yes
Methanothermococcus okinawensis IH1	yes	yes	yes	yes	yes
Methanopyri -> *Methanopyrales* -> *Methanopyraceae*					
Methanopyrus kandleri AV19	yes	yes	yes	yes	yes
Methanomicrobia -> *Methanosarcinales* -> *Methanosaetaceae*					
Methanosaeta concilii GP6	yes	yes	yes	yes	yes
Methanosaeta harundinacea 6Ac	yes	yes	yes	yes	yes
Methanosaeta thermophila PT	yes	yes	yes	yes	yes
Methanomicrobia -> *Methanosarcinales* -> *Methanosarcinaceae*					
Methanococcoides burtonii DSM 6242	yes	yes	yes	yes	yes
Methanohalobium evestigatum Z 7303	yes	yes	yes	yes	yes
Methanohalophilus mahii DSM 5219	yes	yes	yes	yes	yes
Methanolobus psychrophilus R15	yes	yes	yes	yes	yes
Methanomethylovorans hollandica DSM 15978	yes	yes	yes	yes	yes
Methanosalsum zhilinae DSM 4017	yes	yes	yes	yes	yes
Methanosarcina acetivorans C2A	yes	yes	yes	yes	yes
Methanosarcina barkeri Fusaro	yes	yes	yes	yes	yes
Methanosarcina mazei Go1	yes	yes	yes	yes	yes
Methanosarcina mazei Tuc01	yes	yes	yes	yes	yes
Crenarchaeota -> Thermoprotei -> *Desulfurococcales* -> *Desulfurococcaceae*					
Aeropyrum camini SY1 JCM 12091	yes	yes	yes	yes	yes
Aeropyrum pernix K1	yes	yes	yes	yes	yes
Ignicoccus hospitalis KIN4 I	yes	yes	yes	yes §	yes §
Staphylothermus hellenicus DSM 12710	yes	yes	yes	yes	yes
Staphylothermus marinus F1	yes	yes	yes	yes	yes
Crenarchaeota -> Thermoprotei -> *Desulfurococcales* -> *Pyrodictiaceae*					
Hyperthermus butylicus DSM 5456	yes	yes	yes	yes	

Pyrolobus fumarii 1A	yes	yes	yes	yes
Crenarchaeota -> Thermoprotei -> *Fervidicoccales* -> *Fervidicoccaceae*				
Fervidicoccus fontis Kam940	yes	yes	yes	(yes)

Table S1. Taxonomic overview of putative HARP homologs and RNP RNase P components in other species provided at the NCBI database (downloaded on Oct. 6th, 2015; for RnpA entries, the NCBI database of Oct. 2016 was searched in addition). Taxonomic groups are indicated in bold letters. HARP homologs were searched in two iterations based on the Aq_880 reference sequence (first round) and all identified sequences presented herein (second round) using blastp+ (at proteome level) and tblastn+ (at genome level) (7) with an *e* value of 10^{-10}. Purely genomic hits (no protein annotation) are indicated by parentheses. To search for RnpA homologs (protein subunit of bacterial RNA-based RNase P, also termed C5) and Rpp29 (also termed Pop4, subunit of archaeal RNA-based RNase P), we used the reference sets provided by (36). The RNA subunit was located using Infernal (30) with the Rfam v12 models of "Bacterial RNase P class A", "B" and "Archaeal RNase P" (31). All results were aligned and manually inspected for false positives. §, retrieved upon increasing the *e* value from 10^{-10} to 10^{-6}; *: encoded on a plasmid, not on the main chromosome. HARP: Homolog of *Aquifex* RNase P; RNA: bacterial RNase P RNA subunit; RnpA: bacterial RNase P protein subunit; Rpp29, Pop5, Rpp30: archaeal RNase P protein subunits. We have omitted Rpp21 in our searches because we assumed that Rpp21 is present in Archaea when Rpp29 is present, considering that the two function as a binary complex that binds to the S-domain of archaeal RNase P RNA (43) (49). The same pertains to Pop5/Rpp30, forming a binary complex binding to the C-domain of archaeal RNase P RNA, but here we listed homologs of both because we found Pop5/Rpp30 homologs in HARP-encoding bacteria, prompting us to take a deeper look into the presence of Pop5 and Rpp30. The γ-proteobacterium *Methylohalobius crimeensis* was included based on the recent classification study on the PIN domain-like superfamily by (28).

Supplementary Materials and Methods

Purification and enrichment of RNase P activity

Cell lysis using a French press

A frozen pellet (2 g) of *A. aeolicus* cells harvested at late exponential growth phase was resuspended in 20 ml ice-cold buffer A60 (50 mM Tris-HCl, 60 mM NH_4Cl, 10 mM $Mg(OAc)_2$, 6 mM DTT, pH 7.45) by vigorous vortexing. The homogenous cell suspension was filled into a syringe and pressed three times through a cannula (∅ = 0.9 mm). Cells were disrupted by three passages through a French Pressure Cell Press (American Instruments Co.; precooled to 4°C) at 1.000 psi. Cell debris was removed by ultracentrifugation at 125,750 x *g* in a fixed angle rotor at 4°C for 1 h (35,000 rpm using a Ti 70 fixed angle rotor). The lysate was stored at -80°C until use.

Purification by FPLC was performed with an ÄKTA™ *basic 10* (GE Healthcare) at room temperature.

Anion exchange chromatography

Anion exchange chromatography (AEC) was performed using a column packed with Diethylaminoethyl (DEAE) Sepharose Fast Flow (GE Healthcare) to a column volume (CV) of 20 ml. The column was equilibrated with 3 x CV of buffer A60 before 10 ml of filtrated (Filtropur S 0.2 from Sarstedt, Germany) cell lysate was applied to the DEAE column. After washing with 2.25 x CV of buffer A60 the elution was started using a step gradient: at each step, the amount of DEAE elution buffer A1000 (50 mM Tris-HCl, 1 M NH_4Cl, 10 mM $Mg(OAc)_2$, 6 mM DTT, pH 7.45) was increased by 10% at the expense of buffer A60 (100% at the beginning). The flow rate was set to 2 ml/min and the elution volume at each step was 2.2 x CV. At the beginning, 4 ml fractions were collected until step 3. Henceforward, 2 ml fractions were collected. Of each elution fraction, 5 µl were tested for RNase P activity (see below). Fractions with RNase P activity reproducibly eluted in step 3 (30% buffer A1000/70% buffer A60). The fractions with maximum RNase P activity from two independend DEAE purification runs were pooled and concentrated (Amicon® Ultra-15 Ultracel®-10K Centrifugal Filters, Merck Millipore, Germany) at 4°C in a swinging bucket rotor to a final volume of 1.5 - 3 ml. Finally, a 4 M $(NH_4)_2SO_4$ stock solution (pH 7.5) was added to adjust the RNase P sample to a final concentration of 1 M $(NH_4)_2SO_4$.

Hydrophobic interaction chromatography

Hydrophobic interaction chromatography (HIC) was performed using a 5 ml HiScreen Phenyl FF low sub column (GE Healthcare). To reduce the loss of sample during passage through a sterile filter (Filtropur S 0.2 from Sarstedt, Germany), HIC start buffer A2 (50 mM Tris-HCl, 60 mM NH_4Cl, 10 mM $Mg(OAc)_2$, 6 mM DTT, 1 M $(NH_4)_2SO_4$, pH 7.45) was added to the sample to reach a total volume of 10 ml. Before sample loading, the column was equilibrated thoroughly with buffer A2 at a flow rate of 1 - 2 ml/min. After loading, non-interacting sample components were washed out with 3 x CV buffer A2 at a flow rate of 1 - 2 ml/min. Elution was performed with a step gradient using buffer A2 (100% at the beginning) and buffer A60. With each elution step, the proportion of buffer A60 was increased by 20%. The total elution volume of each step was 5 x CV. RNase P activity fractions eluted in step 3 at 0.4 M $(NH_4)_2SO_4$ (40% buffer A2 and 60% buffer A60), in step 4 at 0.2 M $(NH_4)_2SO_4$ (20% HIC buffer A2 and 80% buffer A60) and in step 5 at 0 M $(NH_4)_2SO_4$ (100% buffer A60). The eluted fractions with RNase P activity from each step were pooled separately and designated "$HIC_{0.2}$", "$HIC_{0.4}$" and "HIC_0". To decrease the salt concentration, fractions $HIC_{0.2}$ and $HIC_{0.4}$ were dialyzed (ZelluTrans dialysis membranes, MWCO 12 - 14 kDa from Roth, Germany) overnight at 4°C against the 10 to 15-fold sample volume of buffer A60 (three replacements with fresh buffer). For further purification, samples $HIC_{0.4}$, $HIC_{0.2}$ and HIC_0 were

concentrated (Amicon® Ultra-15 Centrifugal Filters Ultracel®-10K; Merck Millipore) to final volumes of 500 to 750 µl, respectively. Concentrated $HIC_{0.4}$ and $HIC_{0.2}$ fractions were further purified separately by size exclusion chromatography (SEC). Ten µl of the concentrated HIC_0 sample were directly analyzed by mass spectrometry (pooled and concentrated fractions from 16 HIC purifications, total volume of 1 ml). 3 µl of the concentrated HIC_0 fraction and 1 - 2 µl of the dialyzed and concentrated $HIC_{0.4}$ and $HIC_{0.2}$ fractions were tested for RNase P activity in parallel.

Size exclusion chromatography

$HIC_{0.4}$ and $HIC_{0.2}$ fractions from two and four separate HIC purifications, respectively, were pooled and concentrated by centrifugal filters (Amicon Ultra-2 mL, Ultracel 10K; Merck Millipore) to final volumes of 125 - 150 µl. Then, the concentrated samples were filtrated through centrifugal filters (Ultrafree-MC, GV 0.22 µm; Merck Millipore) before separate loading on Superose 6 10/300 GL columns (24 ml, GE Healthcare) equilibrated with elution buffer. Elution was performed at a flow rate of 0.3 ml/min with a 1.25-fold column volume (30 ml) of buffer A60 ($HIC_{0.2}$ samples) or buffer A260 ($HIC_{0.4}$ samples; 50 mM Tris-HCl, 260 mM NH_4Cl, 10 mM $Mg(OAc)_2$, 6 mM DTT, pH 7.45). Eluates were collected in fractions of 0.5 ml. Fractions with RNase P activity eluting from Superose 6 columns loaded with $HIC_{0.4}$ or $HIC_{0.2}$ samples were designated "$SEC_{0.4}$" and "$SEC_{0.2}$" fractions, respectively. After sample injection, several aliquots were directly taken from the 0.5 ml fractions eluting between 9 and 20 ml. Thereof, 10-16 µl were withdrawn and tested for RNase P activity after supplementation with $Mg(OAc)_2$ to a final concentration of 10 mM, 40 µl were taken for determining the protein concentration (Bradford assay), 15 µl for SDS-PAGE and 25 µl for mass spectrometry.

Step gradient SDS-PAGE

Aliquots of SEC fractions containing RNase P activity were analyzed by 20% SDS-PAGE in the order of their elution from the SEC column. According to the strength of RNase P activity, SEC fractions were classified as having low or no activity (+/-), increasing or decreasing RNase P activity (+) or maximum activity (++). As mentioned above, 15 µl and 25 µl aliquots of fractions from each category were analyzed by step gradient SDS-PAGE and mass spectrometry, respectively.

For SDS-PAGE, the discontinuous gel system of Laemmli (24) was used. 4x separation gel buffer (1.5 M Tris-HCl pH 8.8, 0.6 % SDS) was mixed with different amounts of Rotiphorese® Gel 30 (solution of acrylamide/bisacrylamide with 0.8 % bisacrylamide, ratio 37.5 : 1; from Roth, Germany) to obtain gel solutions containing 1x separation gel buffer and

15, 13, 11, 9, 8 or 7% polyacrylamide (PAA). Six separation gel layers of equal height were poured onto each other (15% at the bottom, 7% at the top) after the previous layer had polymerized. Finally, a 4% stacking gel was poured onto the top containing 1x stacking gel buffer (0.5 M Tris-HCl pH 6.8, 0.6 % SDS) and 4% PAA. 15 µl sample aliquots were mixed with 5 µl of 4x protein sample buffer (4% (w/v) SDS, 20% (w/v) glycerol, 5% (w/v) 2-mercaptoethanol, 160 mM Tris-HCl pH 6.8 and 0.04% (w/v) bromophenol blue) and heated to 95°C for 4 min before gel loading. Electrophoresis was performed in 1x running buffer diluted from a 10x running buffer stock (Rotiphorese® 10x SDS-PAGE; Roth, Germany) immediately before electrophoresis. The gel was run until bromophenol blue had almost reached the bottom of the gel. Gels were stained with Coomassie Brilliant Blue G250 as described by (10). Bands of interest were excised with a sterile scalpel and analyzed by mass spectrometry.

Qualitative and quantitative mass spectrometry analysis

Probes prepared from gel slices: After staining the SDS gel with colloidal Coomassie (10), bands of interest were cut out of the gel using a sterile scalpel. After destaining, samples were digested "in-gel" by the addition of Sequencing Grade Modified Trypsin (Promega) overnight at 37°C.

Liquid probes: Mass spectrometric analysis of liquid samples was performed with 10 µl of concentrated fraction HIC_0 and 25 µl each of the elution fractions $SEC_{0.2}$ and $SEC_{0.4}$. For quantitative ($SEC_{0.2}$ and $SEC_{0.4}$) or qualitative (HIC_0) mass spectrometric analysis the liquid samples were digested with Sequencing Grade Modified Trypsin (Promega) at 37°C overnight.

The mass spectrometric analysis of the samples was performed using an Orbitrap Velos Pro mass spectrometer (Thermo Scientific). An Ultimate nanoRSLC-HPLC system (Dionex), equipped with a custom 20 cm x 75 µm C18 RP column filled with 1.7 µm beads was connected online to the mass spectrometer through a Proxeon nanospray source. Depending on sample concentration, 1 - 15 µl of the tryptic digest were injected onto a C18 pre-concentration column. Automated trapping and desalting of the sample was performed at a flow rate of 6 µl/min using 0.05% formic acid in demineralized and deionized water as solvent.

For separation of the tryptic peptides the following gradient of solvent A (0.05% formic acid in demineralized and deionized water) and solvent B (80% acetonitrile/0.045% formic acid) was performed at a flow rate of 300 nl/min: After holding 4% B for 5 min, a linear gradient to 45% B within 30 min was applied, followed by a linear increase to 95% solvent B within the next 5 min. The column was connected to a stainless steel nanoemitter (Proxeon, Denmark) and the eluent was sprayed directly towards the heated capillary of the mass

spectrometer using a potential of 2300 V. A survey scan with a resolution of 60000 within the Orbitrap mass analyzer was combined with at least three data-dependent MS/MS scans with dynamic exclusion for 30 s, either using CID with the linear ion-trap or HCD combined with orbitrap detection at a resolution of 7500.

Data analysis was performed using Proteome Discoverer (Thermo Scientific) with SEQUEST (11) and Mascot (Matrix Science, version 2.2) search engines, employing either the Swiss-Prot (4) or NCBI (32) databases.

For relative quantification of single proteins in liquid SEC fractions, 50 ng cytochrome *c* was added as internal standard.

In vitro transcription of *T. thermophilus* ptRNA^{Gly}, *E. coli* RNase P RNA and *B. subtilis* 6S-1 RNA

All RNAs were synthesized by *in vitro* run-off transcription using T7 RNA polymerase (14) (protocol 1) and linearized plasmid DNAs as template (see Table S2). Transcription products were first subjected to phenol extraction using Roti®-Aqua-Phenol (Roth, Germany), followed by chloroform extraction and isopropanol precipitation for 1-2 h at -20°C (addition of 1 volume isopropanol, $^1/_{10}$ volume 3 M NaOAc (pH 5.0) and $^1/_{100}$ volume 20 mg/ml (w/v) glycogen). After centrifugation (60 min at 13,800 x *g* at 4°C) the supernatant was discarded and the pellet was solved in ddH_2O after air-drying. Next, the *in vitro* transcript was purified by 8% denaturing (8 M urea) PAGE gels (in 1x TBE buffer) and the RNA band of interest was excised from the gel after UV shadowing using a sterile scalpel. The gel slice was eluted overnight at 8°C under shaking at 900 rpm (Thermomixer, Eppendorf, Germany) in elution buffer (1 M NaOAc, pH 5.0) before the RNA was finally precipitated by isopropanol as described above.

Table S2: Plasmids used as template for *in vitro* transcription.

in vitro transcribed RNA	plasmid template	linearization	reference
T. thermophilus ptRNA^{Gly}	pSBpt3´hh	Bam HI	(6)
E. coli RNase P RNA	pDW98	Bsa AI	(19)
B. subtilis 6S-1 RNA	pBB-6S-1	Hind III	(5)

Dephosphorylation, 5'-phosphorylation and 5'-[^{32}P]-endlabeling of RNA

In vitro transcripts containing a 5´-triphosphate group were dephosphorylated prior to phosphorylation or 5'-endlabeling. The gel-purified transcripts (1 µg/µl) were incubated in the supplied 1x reaction buffer with 0.3 U/µl thermosensitive alkaline phosphatase (FastAP, Thermo Scientific) at 37°C for 30 min. The enzyme was subsequently inactivated by heating at 75°C for 5 min and the dephosphorylated RNAs were precipitated with ethanol.

RNAs carrying a 5'-monophosphate group were generated by incubation of dephosphorylated RNA (end concentration: 3.5 pmol/µl) in 1x reaction buffer C (50 mM Tris-HCl pH 7.6, 10 mM $MgCl_2$, 5 mM DTT, 0.1 mM spermidine) with 0.5 U/µl T4 polynucleotide kinase (T4 PNK, Thermo Scientific) and 5 mM ATP for 60 min at 37°C. For downstream applications, the 5'-monophosphorylated RNA was extracted first with phenol (Roti®-Aqua-Phenol, Roth), and subsequently with chloroform, precipitated with ethanol and finally dissolved in ddH_2O. For 5'-[^{32}P]-endlabeling, 10-20 pmol dephosphorylated pre-tRNA was incubated with 10 U T4 PNK (Thermo Scientific) and 3 µl [γ^{32}P]-ATP (10 mCi/ml; 3000 Ci/mmol) in 15 µl 1x reaction buffer C (see above) for 60 min at 37°C. The reaction was stopped by addition of 2x RNA sample buffer (2x TBE buffer, 2.6 M urea, 66% deionized formamide, 0.02% [w/v] bromophenol blue and 0.02% [w/v] xylene cyanol blue) and the sample was loaded onto an 8% PAA gel containing 8 M urea for gel purification. After electrophoresis, the radioactively labeled RNA was localized by autoradiography and excised for elution in 1 M NaOAc (pH 5.0) at 8°C overnight under shaking (900 rpm, Thermomixer). After ethanol precipitation the RNA was dissolved in ddH_2O and stored at -20°C.

Processing assays

Partially purified A. aeolicus fractions

The RNase P activity test was performed in a total volume of 20 µl buffer A4.5 (50 mM Tris-HCl pH 7.45, 60 mM NH_4Cl, 6 mM DTT, 4.5 mM $Mg(OAc)_2$) containing 1-16 µl of partially purified cell fraction and trace amounts (< 1 nM, 3,000 Cherenkov cpm ≈ 10, 000 dpm) of 5'-[^{32}P]-endlabeled ptRNA^{Gly} from *Thermus thermophilus*. The cell fractions were preincubated in buffer A4.5 for 5 min at 37°C. The 5'-[^{32}P]-endlabeled pre-tRNA substrate was preincubated in parallel in buffer A4.5 for 5 min at 55°C and 25 min at 37°C unless stated otherwise. Immediately after preincubation, the activity assays were started by mixing substrate solution (4 µl) and cell fraction (16 µl) followed by incubation at 37°C for 15 to 60 min. The reactions were stopped by addition of an equal volume 2x RNA sample buffer (see above) and reaction products were separated by 20% denaturating (8 M urea) PAGE. After electrophoresis, substrate and cleavage products were visualized and quantified by phosphorimaging using a Bio-Imaging Analyzer FLA3000–2R (Fujifilm) and the analysis software AIDA (Raytest) as described (50).

Activity assay with recombinant Aq_880 variants

Enzymatic activity of *A. aeolicus* Aq_880 and mutants thereof (see Fig. S19 and S20) was analyzed in buffer F (50 mM Tris-HCl pH 7.0, 20 mM NaCl, 4.5 mM $MgCl_2$, 20 µg/ml BSA, 5 mM DTT; DTT was always freshly added immediately before buffer use) at 37°C under single-turnover conditions. Enzyme and substrate solutions were preincubated separately, enzyme for 5 min at 37°C and substrate for 5 min at 55°C and 25 min at 37°C, both in buffer F. The final concentrations were 50 nM enzyme and < 1 nM substrate (5'-[^{32}P]-endlabeled ptRNA^{Gly}).

Determination of single-turnover kinetic parameters for pre-tRNA^{Gly} processing by Aq_880

Trace amounts (< 1 nM) of 5'-[^{32}P]-endlabeled *Thermus thermophilus* pre-tRNA^{Gly} were preincubated in buffer F (50 mM Tris-HCl pH 7.0, 20 mM NaCl, 4.5 mM $MgCl_2$, 20 µg/ml BSA, 5 mM DTT; DTT was always freshly added immediately before buffer use) for 5 min at 55°C and 25 min at 37°C. Aq_880 (varied between final concentrations of 5 and 100 nM) was preincubated separately for 5 min at 37°C in buffer F. Reactions were started by combining 16 µl enzyme and 4 µl substrate mix, and aliquots of 4 µl were withdrawn at different time points, such that the first three points were below 70% substrate conversion; reactions were stopped by adding an equal volume 2x RNA sample buffer. Samples were subjected to 20% denaturing (8 M urea) PAGE. The 5'-[^{32}P]-labeled pre-tRNA substrate and the 5'-cleavage product were quantified with a Bio-Imaging Analyzer FLA3000–2R (Fujifilm) and the analysis software AIDA (Raytest). First-order rate constants of cleavage (k_{obs}) were calculated by nonlinear regression analysis (Grafit 5.0.13) fitting the data to the equation $f_{cleaved} = f_{endpoint} (1 - e^{-(k_{obs})t})$, where $f_{cleaved}$ = fraction of pre-tRNA cleaved, t = time, $f_{endpoint}$ = maximum cleavable fraction of pre-tRNA; based on mean k_{obs} values derived from 3-6 independent experiments for each Aq_880 concentration, the kinetic parameters $K_{m(sto)}$ and k_{react} were calculated by fitting the data to the equation $k_{obs} = k_{react}$ x [Aq_880] / ($K_{m(sto)}$ + [Aq_880]); $K_{m(sto)}$ is the enzyme concentration at the half-maximal rate of cleavage and k_{react} is the maximum single-turnover rate (6).

Determination of multiple-turnover kinetic parameters for pre-tRNA^{Gly} processing by Aq_880

Experiments were performed as for the single turnover, except that the final Aq_880 concentration was kept constant at 1 nM and the substrate was varied between 5 and 200 nM.

E. coli and B. subtilis RNase P holoenzyme and E. coli P RNA-alone assays

Enzymatic activity of *E. coli* and *B. subtilis* RNase P holoenzymes (final concentrations: 4 - 50 nM) was analyzed in buffer F (see above) at 37°C unless stated otherwise. For RNase P holoenzyme assays, the P RNA was preincubated for 5 min at 55°C and 5-30 min at 37°C in buffer F followed by incubation with P protein for 5 min at 37°C to reconstitute the holoenzyme. 5'-[^{32}P]-endlabeled substrate was preincubated in parallel in the same buffer (5 min at 55°C and 25 min at 37°C) before mixing 16 µl of enzyme and 4 µl of substrate solution to start the reaction.

For *E. coli* P RNA-alone reactions in Fig. S2, S4, S7 and S9, 4.5 pmol *E. coli* P RNA were incubated in 16 µl buffer A0 (50 mM Tris-HCl pH 7.45, 60 mM NH_4Cl, 6 mM DTT) supplemented with 10 mM $Mg(OAc)_2$ for 5 min at 37°C. In parallel, trace amounts of 5'-[^{32}P]-endlabeled pre-tRNA^{Gly} (4 µl) were preincubated for 5 min at 55°C and subsequently for 25 min at 37°C under the same conditions. Reactions were started by combining 16 µl enzyme and 4 µl substrate mix. After 30-60 min of incubation at 37°C, the reaction was stopped by adding an equal volume of 2x RNA sample buffer.

Thermostability test for Aq_880 and E. coli RNase P

Aq_880 (50 nM) or *E. coli* RNase P holoenzyme (50 nM) were preincubated for 10 min at 85°C in buffer F (50 mM Tris-HCl pH 7.0, 20 mM NaCl, 4.5 mM $MgCl_2$, 20 µg/ml BSA, 5 mM DTT; DTT was always freshly added immediately before buffer use), followed by slow (1.8°C/min) cooling to 37°C and incubation for another 5 min at 37°C. In parallel, trace amounts (< 1 nM) of 5'-[^{32}P]-endlabeled pre-tRNA^{Gly} from *T. thermophilus* were preincubated for 5 min at 55°C and 25 min at 37°C under the same buffer conditions. Processing reactions were started by combining 16 µl enzyme solution and 4 µl substrate solution. After incubation for 30–45 min at 37°C, the reaction was stopped by addition of an equal volume 2x RNA sample buffer. Reaction products were separated by 20% denaturating (8 M urea) PAGE and substrate and cleavage product were visualized and quantified by phosphorimaging as described above.

Pretreatment with micrococcal nuclease (MN)

The processing activity of different recombinant RNase P enzymes was investigated after treatment with micrococcal nuclease (MN). The analyzed enzymes and their final concentrations in the activity assay were 550 nM *A. thaliana* PRORP1, 125 nM *A. aeolicus* Aq_880, 50 nM *E. coli* holoenzyme and 150 nM *E. coli* P RNA. Additionally, the effect of MN treatment on a mixture of 150 nM *E. coli* P RNA plus 125 nM *A. aeolicus* Aq_880 was tested. The RNase P enzyme/enzyme mix was incubated in 17 µl buffer G (50 mM Tris-HCl pH 7.0, 20 mM NaCl, 4.12 mM $CaCl_2$, 20 µg/ml BSA, 5 mM DTT) supplemented with $MgCl_2$ and

either 1 µl MN (Thermo Scientific, 300 U/µl) or 1 µl ddH_2O (control) for 20 min at 37°C/800 rpm in a thermomixer (Eppendorf, Germany). The final Mg^{2+} concentration in the cleavage reaction was 4.5 mM for *A. thaliana* PRORP1 and *A. aeolicus* Aq_880, 10 mM for the *E. coli* holoenzyme and 100 mM for *E. coli* P RNA. The MN activity was stopped by adding 3 µl 0.2 M EGTA (pH 8.0) to the enzyme mix. Prior to reaction start, the enzyme mix was incubated for another 5 min at 37°C. In parallel to MN treatment of the enzyme solution, 7 nM of 5'-[^{32}P]-endlabeled $ptRNA^{Gly}$ from *T. thermophilus* supplemented with 3.5 µM carrier RNA (*in vitro* transcribed *B. subtilis* 6S-1 RNA) were preincubated for 5 min at 55°C and 20 min at 37°C in buffer F (see above). The reaction was started by combining 16 µl enzyme and 4 µl substrate solution. After incubation for 45 min at 37°C the reaction was stopped by addition of an equal volume 2x RNA sample buffer and the enzymatic activity was determined as described above.

Cell lysate supplemented with recombinant proteins

The influence of recombinant *A. aeolicus* proteins Aq_707, Aq_221 (PNPase) and Aq_880 on pre-$tRNA^{Gly}$ cleavage by the endogenous RNase P activity of partially purified *A. aeolicus* cell lysates (Fig. 2A and S13) was analyzed as follows: recombinant Aq_707 (final concentration: 2.5 µM), Aq_221 (final concentration: 1.5 µM) or Aq_880 (final concentration: 4.2 µM) were combined with $HIC_{0.4}$ eluate (3.7 µg protein; see Fig. S3) in a volume of 20 µl and preincubated for 5 min at 37°C in buffer A0 (50 mM Tris-HCl pH 7.45, 60 mM NH_4Cl, 6 mM DTT) supplemented with 4.5 mM $Mg(OAc)_2$. In parallel, substrate mix containing 164 nM 5'-phosphorylated and trace amounts of 5'-[^{32}P]-endlabeled pre-$tRNA^{Gly}$ in a total volume of 7 µl buffer A0 supplemented with 4.5 mM $Mg(OAc)_2$ was preincubated for 5 min at 55°C followed by 25 min at 37°C. The reaction was started by combining 16 µl preincubated enzyme and 4 µl preincubated substrate solution (final substrate concentration: 33 nM). Reaction aliquots of 4 µl were taken at different time points (1, 5, 10, 30 and 60 min) and were immediately added to an equal volume of 2x RNA sample buffer to stop the cleavage reaction. The enzymatic activity was analyzed by 20% denaturating (8 M urea) PAGE as described above. As control activity, preassembled (45) *B. subtilis* RNase P holoenzyme (10 nM) was analyzed in KN buffer supplemented with 4.5 mM Mg^{2+}.

Aq_880 supplemented with total RNA

The activity of recombinant Aq_880 (final concentration: 50 nM) was analyzed in the presence of total RNA from *A. aeolicus* (final concentration 20 ng/µl; prepared by acetic acid plus phenol/chloroform extraction or phenol/chloroform extraction; see below) at 37°C or 70°C. For performing the processing assay at 37°C, Aq_880 was preincubated for 5 min at 37°C in the presence of total RNA in buffer F. For performing the processing assay at 70°C,

the total RNA was preincubated 5 min at 70°C in buffer F before Aq_880 was added; thereafter, the mixture was incubated for another 10 min at 70°C. In parallel, < 1 nM 5'-[^{32}P]-endlabeled pre-tRNA^{Gly} was incubated for 10 min at 70°C under the same buffer conditions. The reactions were started by combining preincubated enzyme and substrate solution. After 1, 2, 5 and 30 min incubation at 37°C or 70°C, aliquots were taken and analyzed by 20% denaturing PAGE as described before.

Activity assay with other bacterial RNase P RNAs

Enzymatic activity of chimeric holoenzymes composed of bacterial P RNA from *Thermodesulfatator indicus* or *E. coli* (= positive control), and P protein from *B. subtilis* was analyzed in buffer KN (20 mM HEPES-KOH, pH 7.4; 150 mM NH_4OAc; 2 mM spermidine; 50 µM spermine; 4 mM ß-mercaptoethanol) supplemented with 4.5 mM $MgCl_2$ at 25°C. First, 0.2 pmol bacterial P RNA was preincubated in a total volume of 15 µl for 5 min at 55°C and 15 min at 25°C before addition of 1 µl (1 pmol) *B. subtilis* P protein. For holoenzyme assembly, the sample was incubated for another 5 min at 25°C. For RNA-alone reactions, 0.5 pmol bacterial P RNA was preincubated in a total volume of 16 µl for 5 min at 55°C and 20 min at 25°C in buffer KN supplemented with 100 mM $MgCl_2$. In parallel, trace amounts (< 1 nM) of 5'-[^{32}P]-endlabeled ptRNA^{Gly} from *T. thermophilus* were preincubated in a total volume of 10 µl for 5 min at 55°C and 20 min at 25°C under the same buffer conditions (KN buffer plus 4.5 or 100 mM Mg^{2+}). Reaction was started by combining 16 µl preincubated enzyme and 4 µl preincubated substrate mix. Aliquots were taken (after 20 s, 1 min, 5 min and 12 min) and analyzed by 20% denaturing PAGE.

Activity assays using other HARP proteins

Activity of HARP proteins was analyzed in buffer F (50 mM Tris-HCl pH 7.0, 20 mM NaCl, 4.5 mM $MgCl_2$, 20 µg/ml BSA, 5 mM DTT) using trace amounts (< 1 nM) of 5'-[^{32}P]-endlabeled *T. thermophilus* pre-tRNA^{Gly}. The latter was preincubated for 5 min at 55°C and 5 min at 37°C. The HARP protein (final concentration 50 nM) was preincubated in parallel in the same buffer for 5 min at 37°C. The reaction was started by combining preincubated enzyme and substrate solutions. Aliquots were taken after 5, 15 and 30 min. Processing reactions were analyzed by 20% denaturing PAGE (see example in Fig. S21).

Construction of bacterial expression vectors for Aq_880

For the expression of an Aq_880 variant containing a C-terminal His tag (= pET28a(+)*_aq880*cHis), the *aq_880* gene was amplified from chromosomal DNA of *A. aeolicus* using the primer pair 630 (5'-AAG *CCA TGG* ATG TGT TCG TTC TCG ACA C-3'; Nco I site in italics) / 631 (5'-CT*C TCG AG*A AAC CTG TGT CTT ACC AAG CTC TC-3'; Xho

I site in italics). The chromosomal DNA was prepared with the DNeasy Tissue Kit (Qiagen) according to the instructions of the manufacturer and the PCR amplification was performed with the Long PCR Enzyme Mix (Thermo Scientific). The DNA product was inserted via the primer-encoded restriction sites Nco I and Xho I into vector pET28a(+) (Novagen). The resulting plasmid pET28a(+)_*aq880*cHis was transformed into *E. coli* Rosetta (DE3) cells. For the *in vivo* complementation studies in *E. coli* strain BW (48) the expression vector pDG_*aq880*cHis was constructed. Therefore, the *aq_880* gene including the sequences for the C-terminal His tag and the T7 terminator sequence at the 3'-end was PCR-amplified from expression vector pET28a(+)_*aq880*cHis using the primer pair 645 (5'-AG*C CCG GG*C ATG GAT GTG TTC GTT CTC GAC AC-3'; Sma I site in italics) / 646 (5'-AG*G CAT GC*A TCC GGA TAT AGT TCC TCC TTT CAG-3'; Sph I site in italics). The PCR fragment was inserted via the primer-encoded restriction sites Sma I and Sph I into vector pDG148(S/X) (13). In addition, for all Aq_880 variants, pDG148(S/X) derivatives were constructed that encoded the proteins without His-tag. For this purpose, primer 646 was replaced with primer 054a_Aq_pDG_no His (5'- TTT *GCA TGC* **TTA** AAA CCT GTG TCT TAC CAA GC-3'; stop codon in bold, Sph I site in italics).

Construction of expression vectors for Aq_880 variants D160A, D138A, D144A and D142A

Plasmids for the production of Aq_880 variants containing unique aspartate-to-alanine mutations were produced from vector *pET28a(+)::aq880cHis* by site-directed mutagenesis according to the protocol of the QuikChange® XL Site-Directed Mutagenesis Kit (Agilent Technologies). Yet, for PCR reactions we used the *Pwo* DNA polymerase (Peqlab). The primers used for the *in vitro* mutagenesis are listed in Table S3 below. The Aq_880 variants were expressed and purified as described below for the Aq_880 wild-type protein under "Expression and purification of recombinant proteins".

	Sequence 5´--> 3´
In vitro mutagenesis	
009_Aq880_D142A_for	AATACTCGACAGTAAAGAGG**C**CGTGGATGTGCTGCTCCTTGCC
010_Aq880_D142A_rev	GGCAAGGAGCAGCACATCCACG**G**CCTCTTTACTGTCGAGTATT
011_aq880_D160A_for	ACGGGGTTCTCGTTTCGGCGG**C**TGAAGGCCTCAGAACATGGGC
012_Aq880_D160A_rev	GCCCATGTTCTGAGGCCTTCA**G**CCGCCGAAACGAGAACCCCG
013_Aq880D142144A_f	AATACTCGACAGTAAAGAGG**C**CGTGG**C**TGTGCTGCTCCTTGCC
014_Aq880_D142144A_r	GGCAAGGAGCAGCACA**G**CCACG**G**CCTCTTTACTGTCGAGTATT

024_Aq880D138A_for	TCAGGCAGGGAATACTCG**C**CAGTAAAGAGGACGTGG
025_Aq880D138A_rev	CCACGTCCTCTTTACTG**G**CGAGTATTCCCTGCCTGA
026_Aq880D144A_for	AATACTCGACAGTAAAGAGGACGTGG**C**TGTGCTGCTCCTTGCC
027_Aq880D144A_rev	GGCAAGGAGCAGCACA**G**CCACGTCCTCTTTACTGTCGAGTATT
complementation	
645 (forward), Sma I site in italics	AG*C CCG GG*C ATG GAT GTG TTC GTT CTC GAC AC
646 (reverse), for C-His variants, Sph I site in italics	AG*G CAT GC*A TCC GGA TAT AGT TCC TCC TTT CAG
054a_Aq_pDG_no His (reverse), stop codon in bold, Sph I site in italics	TTT *GCA TGC* **TTA** AAA CCT GTG TCT TAC CAA GC

Table S3: Oligonucleotides used for site-directed mutagenesis and complementation analyses in *E. coli* BW. Codon mutations are indicated by bold letters, with the altered codons underlined.

Expression and purification of recombinant proteins

Aq_880 variants carried a C-terminal His tag for purification by Ni-NTA affinity chromatography. Genes for the recombinant proteins were inserted into the expression vector pET28a(+) (Novagen) and were expressed in *E. coli* strain Rosetta (DE3). The Aq_880 variants were either prepared by "*batch*" purification or using the ÄKTApurifier chromatography system (GE Healthcare). Generally, 250-800 ml of "auto induction" LB medium supplemented with 0.05% (w/v) glucose and 0.2% (w/v) lactose (40) were inoculated with a single colony followed by growth overnight at 37°C/200 rpm in an air shaker (GFL, model 3033, Germany). After cell harvest by centrifugation, the cell pellet was resuspended in 10 ml (or 30 ml for ÄKTA purification) NPI-10 buffer (50 mM NaH_2PO_4, 300 mM NaCl, 10 mM Imidazol) and bacteria were lysed by sonication. Cell debris was pelleted by centrifugation for 45 min at 8.000 x g/4°C. For "*batch*" purification 1 ml of Protino® Ni-NTA (Machery-Nagel) was equilibrated with NPI-10 buffer before adding the cleared cell lysate. After rotation overhead for 60-120 min at 4°C the slurry was centrifugated for 2 min at 2,500 x g/4°C, the supernatant was discarded and the matrix was washed with 1 ml buffer NPI-10 (4-6x). For elution, the matrix was incubated 3 to 5 times with 1 ml NPI-250 buffer (50 mM NaH_2PO_4, 300 mM NaCl, 250 mM Imidazol). The eluted fractions were pooled and dialyzed (MWCO 12-14 kDa) against storage buffer (10 mM Tris-HCl pH 8, 100 mM KCl, 0.1 mM EDTA, 3 mM DTT, 50% glycerin, and 10 mM $MgCl_2$ if required). For ÄKTA purification, a 1 ml HisTrap HP (GE Healthcare) column was used. After equilibration with NPI-10 buffer the cleared lysate was loaded onto the column and washed with NPI-10 buffer until the flow

through reached baseline absorption at 254 and 280 nm. Proteins were finally eluted with NPI-250 buffer collecting 1-2 ml fractions. The purity of the preparation was controlled by SDS-PAGE and Coomassie brilliant blue staining. Elution fractions containing the protein were pooled and dialyzed against storage buffer (see above).

The bacterial RNase P proteins from *E. coli* and *B. subtilis* were purified using a N-terminal polyhistidine affinity tag (His-tagged peptide leader: MRGSHHHHHHGS). The His-tagged proteins are encoded in plasmid pQE-30 and were expressed in *E. coli* strain JM109. Expression and purification were performed as described previously (35) (48).

The PRORP1 gene from *A. thaliana* was cloned into the NcoI/XhoI sites of vector pET28b(+) (Novagen) and was expressed in *E. coli* BL21(DE3). The recombinant variant of PRORP1 lacked the mitochondrial targeting sequence of the native precursor and contained a C-terminal His-tag for affinity chromatography purification as described in (33).

For activity assays, Aq_880 and PRORP1 were diluted in enzyme dilution buffer (30 mM Tris pH 7.8, 30 mM NaCl, 10 % (v/v) gycerol, 10 µg/ml BSA, 1 mM DTT, 0.3 mM EDTA).

RT-PCR analysis

First, the detection limit of *E. coli* P RNA in the RT-PCR assay (Access RT-PCR system kit, Promega) was determined. Different amounts of *in vitro* transcribed *E. coli* P RNA (10 amol, 1 amol, 100 zmol and 10 zmol) were used as template for RT-PCR-amplification with specific primers EcM1-5 (5-GAA GCT GAC CAG ACA GTC GCC GCT TC-3) and EcM1-3 (5-ATC TAG GCC AGC AAT CGC TC-3). *In vitro* transcribed *B. subtilis* 6S-1 RNA (20 pmol) was added to each reaction as carrier RNA. The RT-PCR reaction was performed according to the manufacturer´s protocol. Next, different fractions from the preparation of recombinant Aq_880 and Aq_880[D142] were tested for *E. coli* P RNA contamination, including fractions from "*batch*" and ÄKTA purification: (i) elution fractions after dialysis (each 1.25 pmol protein; the same amount that was used in the activity assays); (ii) flow through fractions (each 2.5 µl; unbound sample washed out before elution) and (iii) cell lysates (each 2.5 µl; soluble cell fractions after sonication). Each sample was filled with ddH_2O to a final volume of 400 µl and was subjected to phenol extraction (Roti®-Aqua-Phenol, Roth) followed by chloroform extraction. After subsequent ethanol precipitation, the air-dried RNA pellet was resolved in 10 µl ddH_2O for RT-PCR analysis (see above). In additional control reactions the reverse transcriptase was omitted. (RT-)PCR products (each 3 µl) were separated on 2% agarose gels and stained with ethidium bromide.

A. aeolicus total RNA preparation

Phenol-chloroform extraction

Total RNA was prepared according to Method 1 ("Extracting RNA three times with hot phenol.") described by (8) using 0.1 g cell pellet from *A. aeolicus*. The lysozyme treatment was omitted.

Acetic acid extraction

Total RNA was prepared from RNase P-enriched *A. aeolicus* $HIC_{0.2}$ and $HIC_{0.4}$ fractions by the "acetic acid extraction" method originally developed for the separation of ribosomal RNA and proteins (17) (18). Shortly, $^1/_{10}$ volume icecold 1 M $Mg(OAc)_2$ and 2 volumes icecold acetic acid were added to the concentrated (Amicon®Ultra 10K, Millipore) *A. aeolicus* cell fraction (130-150 µl) and incubated for 45 min on ice in a shaking device at 200 rpm. Next, RNA and protein were separated by centrifugation for 30 min at 9,600 x *g* / 4°C. The protein-containing supernatant was carefully removed from the pelleted RNA. The RNA pellet was resuspended in the 20-fold volume (relative to the volume of initial RNase P-enriched cell fraction) of buffer AAE/urea (20 mM Tris-HCl pH 7.4, 4 mM $Mg(OAc)_2$, 400 mM NH_4Cl, 0.16 mM EDTA, 6 M urea, 4 mM DTT) and dialyzed against the 10,000-fold volume of AAE/urea buffer at 4°C overnight. Subsequently, the RNA fraction was dialyzed twice against the 5,000-fold volume of urea-free AAE buffer for 45 min. The dialysis was immediately stopped when clouding in the dialysis bag was observed. After dialysis the RNA-containing fraction was first centrifugated for 30 min at 4,000 × *g* / 4°C and then concentrated to the 1.5-fold volume of the initial RNase P-enriched cell fraction using centrifugal filters. Finally, the RNA was precipitated with ethanol, washed twice with 70% ethanol and resuspended in buffer A60 (50 mM Tris-HCl pH 7.45, 60 mM NH_4Cl, 10 mM $Mg(OAc)_2$, 6 mM DTT). For the experiment shown in Fig. S14, the total RNA was further subjected to phenol extraction (Roti®-Aqua-Phenol, Roth), chloroform extraction and ethanol precipitation.

Size exclusion chromatography of recombinant Aq_880

First, the Superose 6 10/300 GL column (24 ml, GE Healthcare) was calibrated using Apoferritin [from horse spleen] (Sigma-Aldrich) and the Gel Filtration Markers Kit (Sigma-Aldrich). After equilibration with buffer S (50 mM Tris-HCl pH 7.45, 150 mM NaCl, 4.5 mM $Mg(OAc)_2$, 5 mM DTT) the standard proteins (bovine serum albumin, alcohol dehydrogenase, β-amylase, carbonic anhydrase, cytochrome *c* and apoferritin; each 0.6 mg) were loaded onto and passed through the column at a flow rate of 0.3 ml/min at room temperature. The elution volume of each standard protein was determined. To find out whether Aq_880 forms oligomers, 1.3 mg recombinant Aq_880 (ÄKTA-purified) was applied to the calibrated column as described for the standard proteins. Before application, the Aq_880 was filtrated

(Ultrafree-MC, GV 0.22 µm, Merck Millipore). The oligomerization state of Aq_880 was inferred from comparing the elution volume of recombinant Aq_880 with the elution volumes of the standard proteins.

Complementation studies

In the *E. coli* strain BW, expression of the essential *rnpB* gene (encoding the RNase P RNA subunit) is under control of an arabinose-inducible promoter (48). Under non-permissive conditions the survival of the cells depends on a functional plasmid-encoded RNase P activity. For *in vivo* analysis, the different pDG148-based expression vectors were introduced into *E. coli* BW cells by transformation of chemically competent cells. For the complementation tests, transformed cells were plated on LB agar plates supplemented with 10 mM arabinose, 100 µg/ml ampicillin and 34 µg/ml chloramphenicol. After incubation overnight at 37°C, single colonies were resuspended in 500 µl LB medium, pelleted in a desktop centrifuge and again resuspended in 500 µl LB medium. 3 to 5 aliquots (each 10 µl) were dropped in parallel onto selective LB agar plates supplemented either with 10 mM arabinose (permissive conditions) or 10 mM glucose (non-permissive conditions). The plates were incubated for 1 to 5 days at 37°C or 30°C. Other HARP genes were analyzed in the same way using gene-specific primers for the construction of corresponding pDG148(S/X) derivatives.

For the complementation studies in *Saccharomyces cerevisiae, aq_880* variants were constructed and amplified by PCR techniques and then cloned into the XbaI/HindIII sites of a derivative of plasmid YEplac181 containing the truncated *S. cerevisiae ADH1* promoter exactly as previously described (47). The previously described plasmid-shuffle system (47) was used to test whether *aq_880* (or its variants) enabled the tester strain with its chromosomal *RPR1* deletion (*rpr1 Δ::kanMX4*) to lose the *RPR1* expression plasmid with the *URA3* marker and thereby survive selection on 5-fluoroorotic acid. Colonies obtained through rescue by Aq_880 or its variant D144A were isolated, regrown, and subsequently applied as spots in 10-fold serial dilution to YPD plates. The growth of the strains was monitored in parallel to a control (rescue by *RPR1*). PCR genotyping was carried out as previously described (42). To verify the presence of *aq_880*, primers flanking the gene in the vector were used (primer *for*, 5'-CCTCGTCATTGTTCTCGTT; primer *rev*, 5'-GGCTCGTATGTTGTGTGGA). All other genotyping primers were described previously (47).

A. aeolicus* proteins identified by mass spectrometry - occurrence of homologs in the *Aquificales

Analyses for the presence of Aq_880 and Aq_707 homologs in the *Aquificales* and particularly in the *Aquificaceae* were performed with BLAST+ (7; *e* value 10^{-5}) and the

genomes published in the NCBI database (34; download 2013-08-05). The classification of the organisms was based on the NCBI taxonomy database.

References

(1) Anantharaman V, Aravind L (2006) The NYN domains: novel predicted RNAses with a PIN domain-like fold. *RNA biology* 3(1):18-27.

(2) Arcus VL, McKenzie JL, Robson J, Cook GM (2010) The PIN-domain ribonucleases and the prokaryotic VapBC toxin–antitoxin array. Protein Eng. Des. Sel. 24(1-2):33-40. doi: 10.1093/protein/gzq081.

(3) Andrews AJ, Hall TA, Brown JW (2001) Characterization of RNase P holoenzymes from *Methanococcus jannaschii* and *Methanothermobacter thermoautotrophicus*. *Biol. Chem*. 382(8):1171-1177. doi: 10.1515/BC.2001.147.

(4) Bairoch A, Apweiler R (2000) The SWISS-PROT protein sequence database and its supplement TrEMBL in 2000. *Nucleic Acids Res.* 28(1):45-48.

(5) Beckmann BM, Burenina OY, Hoch PG, Kubareva EA, Sharma CM, Hartmann RK (2011) In vivo and in vitro analysis of 6S RNA-templated short transcripts in *Bacillus subtilis*. RNA Biol. 8(5):839-849. doi: 10.4161/rna.8.5.16151.

(6) Busch S, Kirsebom LA, Notbohm H, Hartmann RK (2000) Differential role of the intermolecular base-pairs G292-C(75) and G293-C(74) in the reaction catalyzed by *Escherichia coli* RNase P RNA. *J. Mol. Biol.* 299(4):941-951. doi: 10.1006/jmbi.2000.3789.

(7) Camacho C, Coulouris G, Avagyan V, Ma N, Papadopoulos J, Bealer K, Madden TL (2008) BLAST+: architecture and applications. *BMC Bioinformatics* 10:421. doi: 10.1186/1471-2105-10-421.

(8) Damm K, Bach S, Müller KM, Klug G, Burenina OY, Kubareva EA, Grünweller A, Hartmann RK (2015) Impact of RNA Isolation Protocols on Detection by Northern Blotting. *Methods Mol. Biol.* 1296:29-38. doi: 10.1007/978-1-4939-2547-6_4.

(9) Das R, Loss S, Li J, Waugh DS, Tarasov S, Wingfield PT, Byrd RA, Altieri AS (2008) Structural biophysics of the NusB:NusE antitermination complex. *J. Mol. Biol.* 376(3):705-720. doi: 10.1016/j.jmb.2007.11.022.

(10) Dyballa N, Metzger S (2009) Fast and sensitive colloidal coomassie G-250 staining for proteins in polyacrylamide gels. *J. Vis. Exp*. pii: 1431. doi: 10.3791/1431.

(11) Eng JK, McCormack AL, Yates JR (1994) An approach to correlate tandem mass spectral data of peptides with amino acid sequences in a protein database. *J. Am. Soc. Mass Spectrom.* 5(11):976-989. doi: 10.1016/1044-0305(94)80016-2.

(12) Gough J, Karplus K, Hughey R, Chothia C (2001) Assignment of homology to genome sequences using a library of hidden Markov models that represent all proteins of known structure. *J. Mol. Biol.* 313(4):903-919. doi: 10.1006/jmbi.2001.5080.

(13) Gößringer M, Hartmann RK (2007) Function of heterologous and truncated RNase P proteins in *Bacillus subtilis*. *Mol. Microbiol.* **66(3):**801-813. doi: 10.1111/j.1365-2958.2007.05962.x.

(14) Gößringer M, Helmecke D, Köhler K, Schön A, Kirsebom LA, Bindereif A, Hartmann RK (2014) Enzymatic RNA Synthesis Using Bacteriophage T7 RNA Polymerase. *Handbook of RNA Biochemistry Vol. 1*, eds Hartmann RK, Bindereif A, Schön A, Westhof E) (Wiley-VCH), pp 21-27.

(15) Hall TA, Brown JW (2002) Archaeal RNase P has multiple protein subunits homologous to eukaryotic nuclear RNase P proteins. *RNA* 8(3):296-306.

(16) Hall TA, Brown JW (2004) Interactions between RNase P protein subunits in archaea. *Archaea* 1(4):247-254.

(17) Hardy SJ, Kurland CG, Voynow P, Mora G (1969) The ribosomal proteins of *Escherichia coli*. I. Purification of the 30S ribosomal proteins. *Biochemistry*. 8(7):2897-28905.

(18) Hartmann RK, Vogel DW, Walker RT, Erdmann VA (1988) In vitro incorporation of eubacterial, archaebacterial and eukaryotic 5S rRNAs into large ribosomal subunits of *Bacillus stearothermophilus*. *Nucleic Acids Res*. 16(8):3511-24.

(19) Heide C, Pfeiffer T, Nolan JM, Hartmann RK (1999) Guanosine 2-NH_2 groups of *Escherichia coli* RNase P RNA involved in intramolecular tertiary contacts and direct interactions with tRNA. *RNA*. 5(1):102-116.

(20) Holzmann J, Frank P, Löffler E, Bennett KL, Gerner C, Rossmanith W (2008) RNase P without RNA: identification and functional reconstitution of the human mitochondrial tRNA processing enzyme. *Cell* 135(3):462-474. doi: 10.1016/j.cell.2008.09.013.

(21) Howard MJ, Lim WH, Fierke CA, Koutmos M (2012) Mitochondrial ribonuclease P structure provides insight into the evolution of catalytic strategies for precursor-tRNA 5' processing. *Proc. Natl. Acad. Sci. U S A.* 109(40):16149-16154. doi: 10.1073/pnas.1209062109.

(22) Kelley LA, Mezulis S, Yates CM, Wass MN, Sternberg MJE (2015) The Phyre2 web portal for protein modeling, prediction and analysis. *Nat. Protoc.* 10(6):845-858. doi: 10.1038/nprot.2015.053.

(23) Kitamura A, Nishimoto M, Sengoku T, Shibata R, Jäger G, Björk GR, Grosjean H, Yokoyama S, Bessho Y (2012) Characterization and structure of the *Aquifex aeolicus* protein DUF752: a bacterial tRNA-methyltransferase (MnmC2) functioning without the usually fused oxidase domain (MnmC1). *J. Biol. Chem.* 287(52):43950-43960. doi: 10.1074/jbc.M112.409300.

(24) Laemmli UK (1970) Cleavage of structural proteins during the assembly of the head of bacteriophage T4. *Nature* 227(5259):680-685.

(25) Lechner M, Nickel AI, Wehner S, Riege K, Beckmann BM, Hartmann RK, Marz M (2014) Genomewide comparison and novel ncRNAs of *Aquificales*. *BMC Genomics* 15:522. doi: 10.1186/1471-2164-15-522.

(26) Marszalkowski M, Teune JH, Steger G, Hartmann RK, Willkomm DK (2006) Thermostable RNase P RNAs lacking P18 identified in the *Aquificales*. *RNA* 12(11):1915-1921. doi: 10.1261/rna.242806.

(27) Marszalkowski M, Willkomm DK, Hartmann RK (2008) 5'-end maturation of tRNA in *Aquifex aeolicus*. *Biol. Chem.* 389(4):395-403. doi: 10.1515/BC.2008.042.

(28) Matelska D, Steczkiewicz K, Ginalski K (2017) Comprehensive classification of the PIN domain-like superfamily. *Nucleic Acids Res.* 2017 May 31. doi: 10.1093/nar/gkx494. [Epub ahead of print].

(29) Murzin AG, Brenner SE, Hubbard T, Chothia C (1995) SCOP: a structural classification of proteins database for the investigation of sequences and structures. *J. Mol. Biol.* 247(4):536-540. doi: 10.1006/jmbi.1995.0159

(30) Nawrocki EP, Eddy SR (2013) Infernal 1.1: 100-fold faster RNA homology searches. *Bioinformatics*. 29(22):2933-2935. doi: 10.1093/bioinformatics/btt509.

(31) Nawrocki EP, Burge SW, Bateman A, Daub J, Eberhardt RY, Eddy SR, Floden EW, Gardner PP, Jones TA, Tate J, Finn RD (2015) Rfam 12.0: updates to the RNA families database. *Nucleic Acids Res.* 43 (Database issue), D130–D137 (2015). doi: 10.1093/nar/gku1063.

(32) NCBI Resource Coordinators (2014) Database resources of the National Center for Biotechnology Information. *Nucleic Acids Res*. 42, D7-17. doi: 10.1093/nar/gkt1146.

(33) Pavlova LV, Gößringer M, Weber C, Buzet A, Rossmanith W, Hartmann RK (2012) tRNA processing by protein-only versus RNA-based RNase P: kinetic analysis reveals mechanistic differences. *Chembiochem* 13(15):2270-2276. doi: 10.1002/cbic.201200434.

(34) Pruitt KD, Tatusova T, Brown GR, Maglott DR (2012) NCBI Reference Sequences (RefSeq): current status, new features and genome annotation policy. *Nucleic Acids Res.* 40 (Database issue):D130-5. doi: 10.1093/nar/gkr1079.

(35) Rivera-Leon R, Green CJ, Vold BS (1995) High-level expression of soluble recombinant RNase P protein from *Escherichia coli*. *J. Bacteriol.* 177(9):2564-2566.

(36) Rosenblad MA, Lopez MD, Piccinelli P, Samuelsson T (2006) Inventory and analysis of the protein subunits of the ribonucleases P and MRP provides further evidence of homology between the yeast and human enzymes. *Nucleic Acids Res.* 34(18):5145-5156. doi: 10.1093/nar/gk1626.

(37) Shigi N, Sakaguchi Y, Suzuki T, Watanabe K (2006) Identification of two tRNA thiolation genes required for cell growth at extremely high temperatures. *J. Biol. Chem.* 281(20):14296-14306. doi: 10.1074/jbc.M511675200.

(38) Sievers F, Wilm A, Dineen D, Gibson TJ, Karplus K, Li W, Lopez R, McWilliam H, Remmert M, Söding J, Thompson JD, Higgins DG (2011) Fast, scalable generation of high-quality protein multiple sequence alignments using Clustal Omega. *Mol. Syst. Biol.* 7:539. doi: 10.1038/msb.2011.75.

(39) Stagno JR, Altieri AS, Bubunenko M, Tarasov SG, Li J, Court DL, Byrd RA, Ji X (2011) Structural basis for RNA recognition by NusB and NusE in the initiation of transcription antitermination. Nucleic acids research 39(17):7803-7815, doi:10.1093/nar/gkr418.

(40) Studier FW (2005) Protein production by auto-induction in high density shaking cultures. *Protein Expr. Purif.* 41(1):207-234.

(41) Symmons MF, Jones GH, Luisi BF (2000) A duplicated fold is the structural basis for polynucleotide phosphorylase catalytic activity, processivity, and regulation. *Structure* 8(11):1215-1226.

(42) Taschner A, Weber C, Buzet A, Hartmann RK, Hartig A, Rossmanith W. (2012) Nuclear RNase P of Trypanosoma brucei: a single protein in place of the multicomponent RNA-protein complex. Cell Rep. Jul 26;2(1):19-25

(43) Tsai HY, Pulukkunat DK, Woznick WK, Gopalan V. (2006) Functional reconstitution and characterization of *Pyrococcus furiosus* RNase P. *Proc. Natl. Acad. Sci. USA* 103(44):16147-16152.

(44) Vilardo E, Nachbaqauer C, Buzet A, Taschner A, Holzmann J, Rossmanith W (2012) A subcomplex of human mitochondrial RNase P is a bifunctional methyltransferase--extensive moonlighting in mitochondrial tRNA biogenesis. *Nucleic Acids Res.* 40(22):11583-11593 (2012). doi: 10.1093/nar/gks910.

(45) Walczyk D, Gößringer M, Rossmanith W, Zatsepin TS, Oretskaya TS, Hartmann RK (2016) Analysis of the Cleavage Mechanism by Protein-Only RNase P Using Precursor tRNA Substrates with Modifications at the Cleavage Site. *J. Mol. Biol.* 428(24 Pt B):4917-4928. doi: 10.1016/j.jmb.2016.10.020.

(46) Wang MJ, Gegenheimer P (1990) Substrate masking: binding of RNA by EGTA-inactivated micrococcal nuclease results in artifactual inhibition of RNA processing reactions. *Nucleic Acids Res.* 18(22):6625-6631.

(47) Weber C, Hartig A, Hartmann RK, Rossmanith W (2014) Playing RNase P evolution: swapping the RNA catalyst for a protein reveals functional uniformity of highly divergent enzyme forms. PLoS Genet. 7;10(8)

(48) Wegscheid B, Hartmann RK (2006) The precursor tRNA 3'-CCA interaction with *Escherichia coli* RNase P RNA is essential for catalysis by RNase P *in vivo*. RNA. 12(12):2135-2148. doi: 10.1261/rna.188306.

(49) Xu Y, Amero CD, Pulukkunat DK, Gopalan V, Foster MP. (2009) Solution structure of an archaeal RNase P binary protein complex: formation of the 30-kDa complex between *Pyrococcus furiosus* RPP21 and RPP29 is accompanied by coupled protein folding and highlights critical features for protein-protein and protein-RNA interactions. *J. Mol. Biol.* 393(5):1043-1055. doi: 10.1016/j.jmb.2009.08.068.

(50) Brillante N, Gößringer M, Lindenhofer D, Toth U, Rossmanith W, Hartmann RK. (2016) Substrate recognition and cleavage-site selection by a single-subunit protein-only RNase P. Nucleic Acids Res. Mar 18;44(5):2323-36